

## Article

# Relation between Central European Climate Change and Eifel Volcanism during the Last 130,000 Years: The ELSA-23-Tephra-Stack

Frank Sirocko <sup>1,\*</sup>, Frederik Krebsbach <sup>1</sup>, Johannes Albert <sup>1</sup>, Sarah Britzius <sup>1,2</sup>, Fiona Schenk <sup>1</sup>  
and Michael W. Förster <sup>3</sup>

<sup>1</sup> Institute of Geosciences, Johannes-Gutenberg University, 55128 Mainz, Germany

<sup>2</sup> Department of Isotope Geochemistry, Max Planck Institute for Chemistry, 55128 Mainz, Germany

<sup>3</sup> Research School of Earth Sciences, Australian National University, Canberra 2601, Australia

\* Correspondence: sirocko@uni-mainz.de

**Abstract:** The analysis of tephra layers in maar lake sediments of the Eifel shows 14 well-visible tephra during the last glacial cycle from the Holocene to the Eemian (0–130,000 yr b2k). These tephra were analyzed for their petrographic composition, which allows us to connect several tephra to eruption sites. All tephra were dated by application of the ELSA-20 chronology, developed using the late Pleistocene infilled maar lake of Auel and the Holocene lake Holzmaar (0–60,000 yr b2k). We extend the ELSA-20 chronology with this paper for the millennia of 60,000–130,000 yr b2k (ELSA-23 chronology), which is based on the infilled maar lake records from Dehner, Hoher List, and Jungferweiher. The evaluation of the tephra from the entire last glacial cycle shows that all 14 tephra were close to interstadial warming of the North Atlantic sea surface temperatures. In particular, phreatomagmatic maar eruptions were systematically associated with Heinrich events or C-events. These events represent times of warming of the Southern Hemisphere, global sea level rise, and CO<sub>2</sub> increase, which predate the abrupt interstadial warming events of the Northern Hemisphere. This synchronicity indicates a physical relationship between endogenic and exogenic processes. Changes in the lithospheric stress field in response to changes in continental ice loads have already been suggested as a potential candidate to explain the exogenic forcing of endogenic processes. The chronology of volcanic activity in the Eifel demonstrates that intraplate mantle plumes are also affected by the exogenic forcing of endogenic processes.

**Keywords:** Eifel; maar sediments; teprochronology



**Citation:** Sirocko, F.; Krebsbach, F.; Albert, J.; Britzius, S.; Schenk, F.; Förster, M.W. Relation between Central European Climate Change and Eifel Volcanism during the Last 130,000 Years: The ELSA-23-Tephra-Stack. *Quaternary* **2024**, *7*, 21. <https://doi.org/10.3390/quat7020021>

Academic Editor: James B. Innes

Received: 20 December 2023

Revised: 27 March 2024

Accepted: 17 April 2024

Published: 25 April 2024



**Copyright:** © 2024 by the authors. Licensee MDPI, Basel, Switzerland. This article is an open access article distributed under the terms and conditions of the Creative Commons Attribution (CC BY) license (<https://creativecommons.org/licenses/by/4.0/>).

## 1. Introduction

### 1.1. West Eifel Volcanic Field

The West Eifel Volcanic Field (WEVF), located in the middle of central Europe (Figure 1A), has experienced continuous episodes of uplift since the early Eocene, always accompanied by volcanic activity [1–5]. This ongoing volcanic activity during the Late Pleistocene in the Cenozoic period is attributed to the heat anomaly of the Eifel plume, currently located at a depth of 70 km, causing a doming effect in the asthenosphere [6]. Melts originating from the melting zone at the lithosphere–asthenosphere boundary ascend into the lower to middle crust until they reach neutral buoyancy and accumulate in small magma chambers. The connections between these magma chambers and the surface occur along pre-existing faults, as evidenced by the alignment of the WEVF with the major tectonic lineaments of the Rhenish Shield (Figure 1B). The landscape of the Eifel is thus formed on the Grauwacke, limestone, and sandstone of Devonian age, pitted with more than 200 scoria cones and about 70 maar structures. Seven of the maar craters are now lakes characterized by varved sediments, which have attracted paleolimnological research during the last 30 years [7–9].

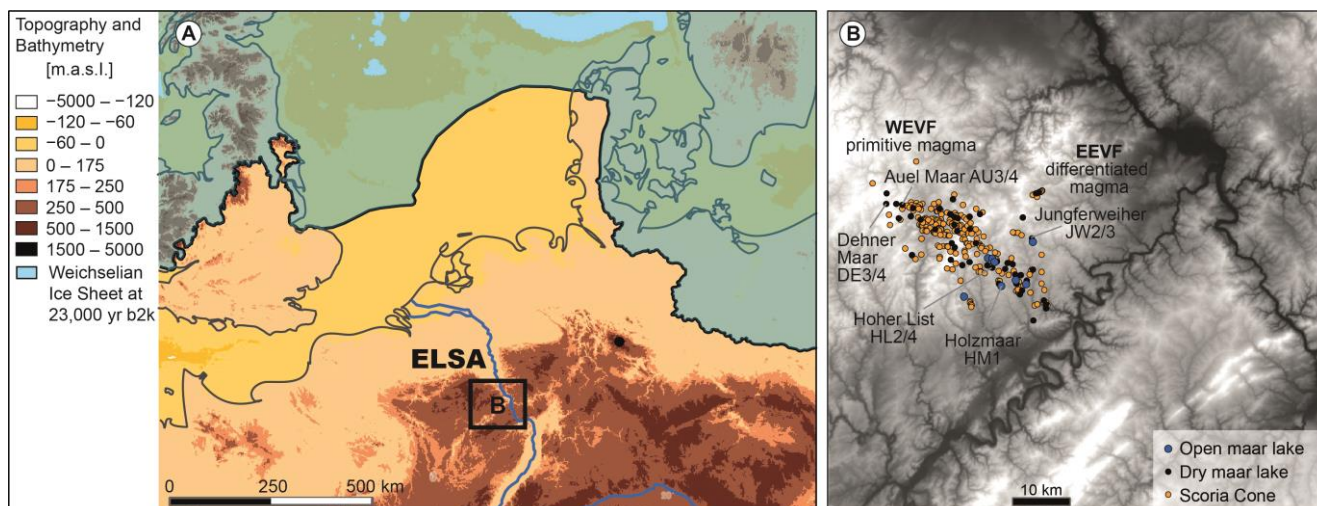
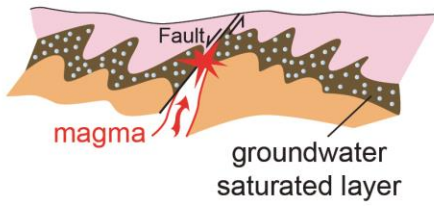


**Figure 1.** (A) Digital Elevation Model of the central European topography during the time of the Last Glacial Maximum sea level lowstand; (B) Digital Elevation Model of the West and East Eifel Volcanic Fields (WEVF and EEVF), together with sites of scoria cones, infilled maar lakes, and open maar lakes [10].

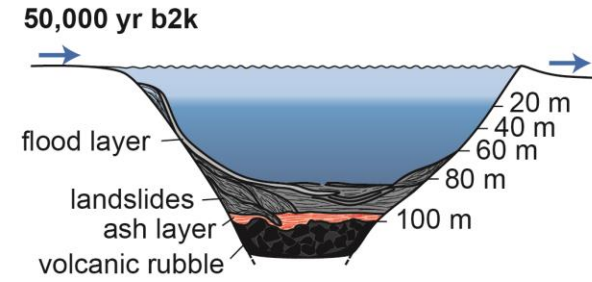
The ascent of highly alkaline magmas, ranging from nephelinitic to basanitic compositions, into the Earth's crust beneath the Eifel volcanic fields resulted in the rapid formation of maar volcanoes through interactions with groundwater and surface water (Figure 2). The explosive nature of phreatomagmatic eruptions is attributed to the abrupt heating of groundwater by rising magma, which causes an expansion of water in the sediment pore space. This process leads to the ejection of the uppermost strata, creating holes several hundred meters deep. The ejected material consists primarily of country rocks comprising up to 90% of the tephra layers, which are mixed with juvenile volcanic minerals, pumice, and scoria. These materials collectively form the tuff wall surrounding a maar. The formation mechanism of these maars, resulting from phreatomagmatic eruptions, has been extensively studied by Büchel et al. [1], Lorenz [11], and Schmincke [12]. The accumulation of numerous phreatomagmatic explosions gives rise to solitary “round holes” in the landscape, reaching widths of up to 1.5 km and depths of 150 m, all rimmed by a tuff wall (Figures 2–5). The tuff exhibits various grain sizes, with the coarsest material found in the tuff wall. It can also be transported over several kilometers by base surges. While the grain size decreases with transport distance, the petrographic composition indicative of phreatomagmatic eruptions remains consistent. These eruptions also expel rock fragments known as xenoliths and minerals, referred to as xenocrysts, throughout the magma's path, primarily representing strata from the uppermost 200 m. Consequently, the base layer of a maar eruption consists of fragments of rocks, which reflect the geological composition at the eruption site; Figure 6 shows the core JW3 from the Jungferweiher as an example, which exhibits a breccia at its base consisting of the fallout from the eruption and collapsed rocks from the crater flanks.

In addition to the volcanic maar lakes, the WEVF also features scoria cones and lava flows resulting from eruptions during the late Quaternary period. Dating of volcanic rocks at the site of eruption has been achieved using techniques such as K/Ar and  $^{40}\text{Ar}/^{39}\text{Ar}$  [13–19]. The resultant ages on the volcanic rocks date the Laacher See eruption to about 13,000 BP (years before present), the Wartgesberg to 32,000 BP, the Mosenberg to 80,000 BP, and the Dümpelmaar to 111,000 BP, revealing volcanic activity during the entire last glacial cycle. The volcanic ash produced by these eruptions differs significantly from the maar tephra in terms of petrographic characteristics. Ash layers found in lake sediments tend to have a very fine grain size and contain pyroxenes, scoria, and pumice, which are also present in maar eruption layers. However, the maar eruption layers consistently contain a high proportion of fragments from the surrounding host rock (Figure 2).

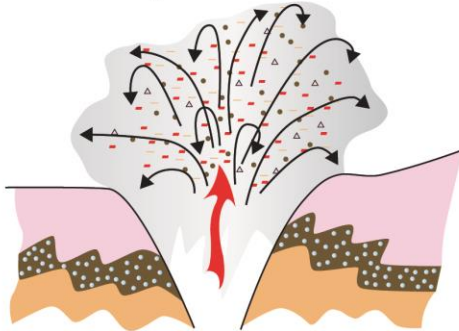
**(A) Phreatomagmatic explosion**



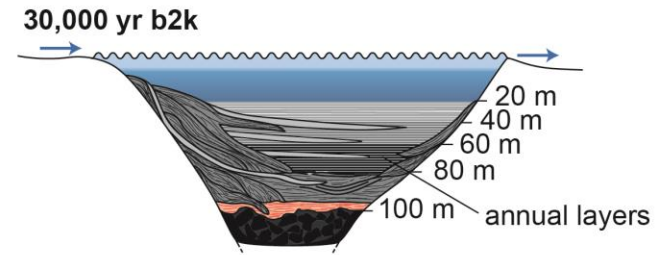
**(D) Maar lake**



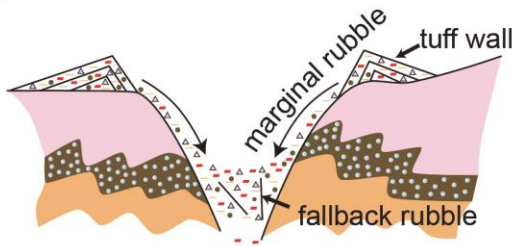
**(B) Crater eruption**



**(E) Infill of the maar lake**



**(C) Maar basin with tuff wall**



**(F) Silted lake - dry maar**

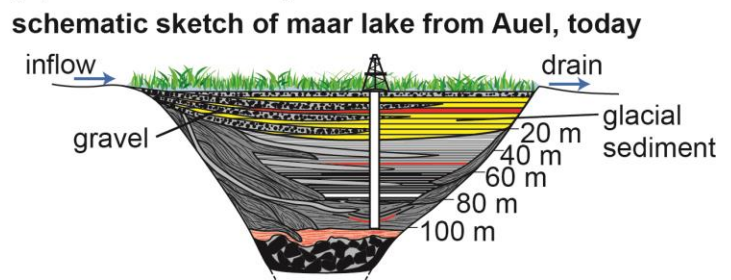


**Figure 2.** Schematic sketch of eruption and sediment fill in the maar basin of Auel.

Maar lakes in the Eifel have diameters ranging from 100 to 1500 m. Drilling data indicate an average sediment filling of approximately one-tenth of the lake diameter. For instance, the 1.5 km wide Jungferweiher maar was filled with 150 m of lake sediment, representing the maximum observed thickness among the ELSA (Eifel Laminated Sediment Archive) drillings (Figure 6). Radiocarbon dating ( $^{14}\text{C}$ ) of the Marine Isotope Stage (MIS) 3 section and optically stimulated luminescence (OSL) dating of MIS 5 have been conducted on many ELSA cores [20]. In this paper, we present the 150 m long lake sediment cores JW2 and JW3 from Jungferweiher with new  $^{14}\text{C}$  dates from a section tuned to Greenland Interstadial (GI) 8. A total of three new  $^{14}\text{C}$  dates were measured on *Picea* needles from separate samples, and date exactly in the expected age around 38,000 yr b2k (years before the year 2000) (Figure 7). These long Jungferweiher cores are of particular importance for this study because they present the MIS 3, MIS 4, and MIS 5 tephra in superposition all in one core covering the time span from approximately 30,000 to 130,000 BP [21]. The average sedimentation rate for the JW cores is 1 mm/year (Figure 6), a value typical for many maar sites. The pollen from the JW3 core has been incorporated in the pollen stack as presented by Britzius et al. [22] (this issue).

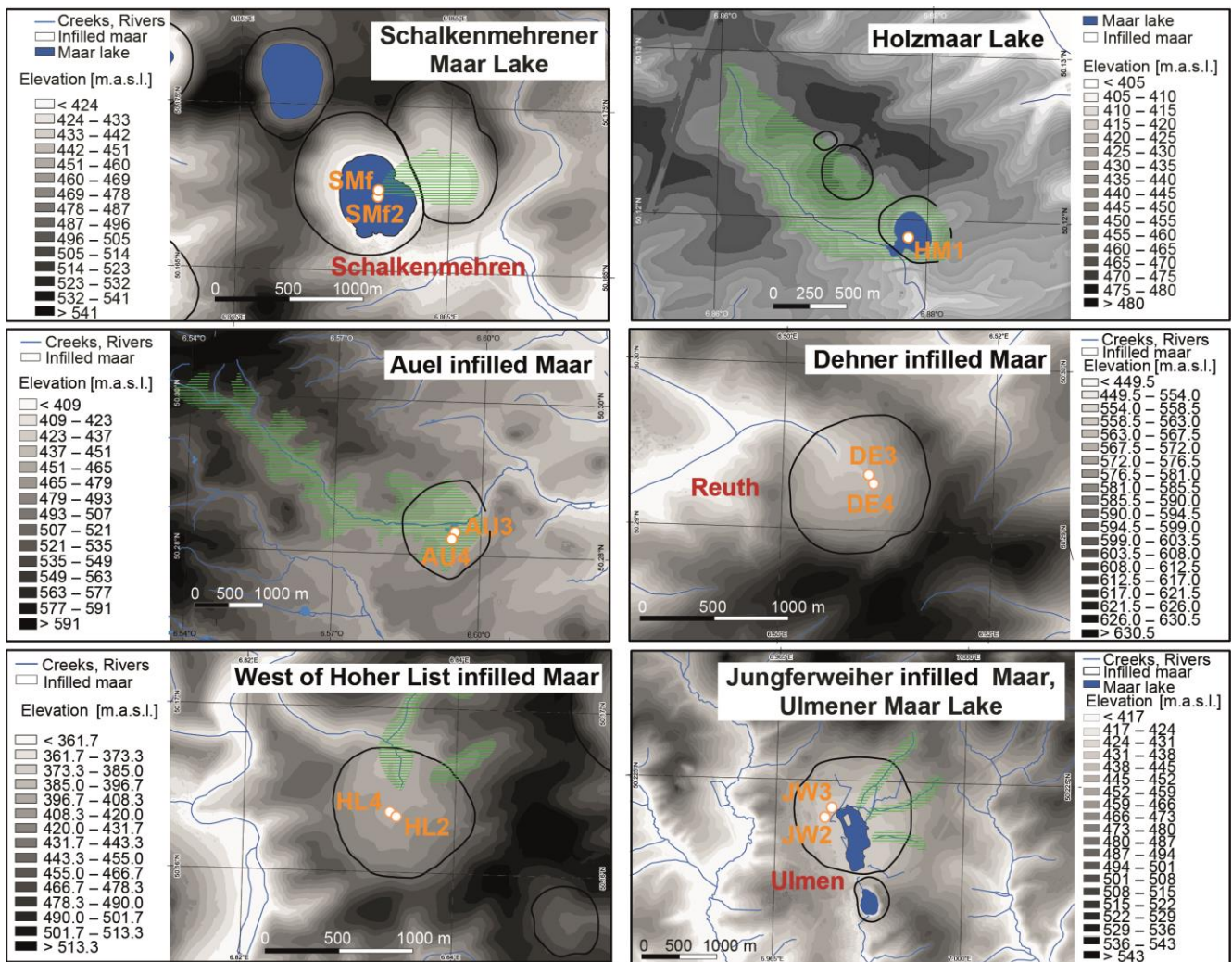


**Figure 3.** Digital Elevation Models of the sites for all cores used for the ELSA-23-Tephra-Stack. Catchment area marked in green.

The ELSA Project was initiated in 1998 and has since systematically scored 50 of the 68 maar sites in the Eifel. Seven of these sites are open lakes with water depths deeper than 20 m, and all others were infilled during the Pleistocene or early Holocene. Twenty infilled maar structures were drilled using Seilkern Technology down to about 100 m, including four of the lakes with a UWITEC piston core, and freeze-core equipment. All of these sediment cores revealed visible layers of tephra, which were petrographically/geochemically characterized and dated by Förster and Sirocko [23] and Förster et al. [24].

These cores reveal  $C_{org}$  variations with a succession of warming events almost identical to the Greenland/North Atlantic temperature variations (Figures 8 and 9; age models of the cores in Figure 7). Warming events in Greenland are called Greenland Interstadials (GIs), and cold phases are called Greenland Stadials (GSs). The very coldest phases have been named Heinrich events (H), when the North Atlantic was covered with drifting icebergs from the decay of the North American ice sheet.



**Figure 4.** Aerial photograph of a typical Eifel volcano, a scoria cone (copyright University of Mainz).



**Figure 5.** Photo of a maar lake (A) (Weinfelder and Schalkenmehrener Maar lake) and an infilled maar lake (B) (west of Hoher List) with drilling equipment (C,D) (copyright University of Mainz).

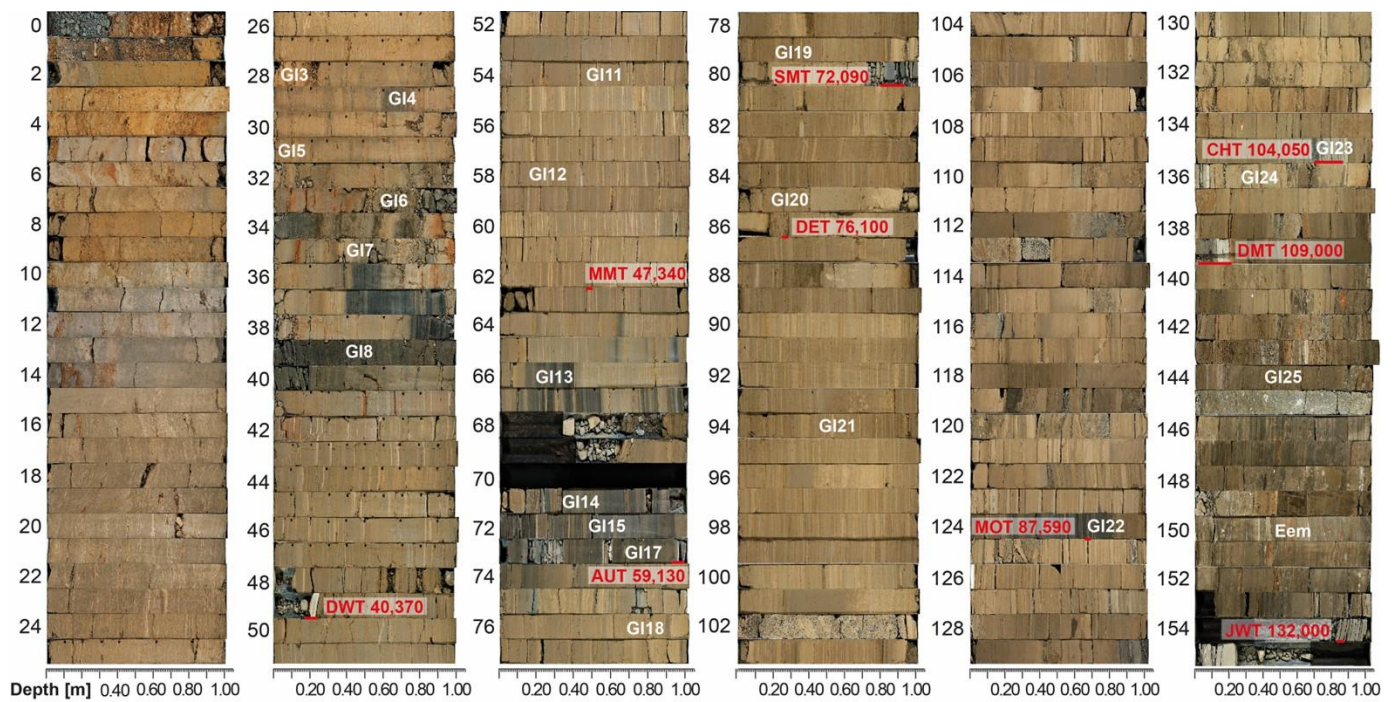


Figure 6. Photo of sediment core JW3 from the Jungferweiher. Tephra are marked in red and interstadial sections in white.

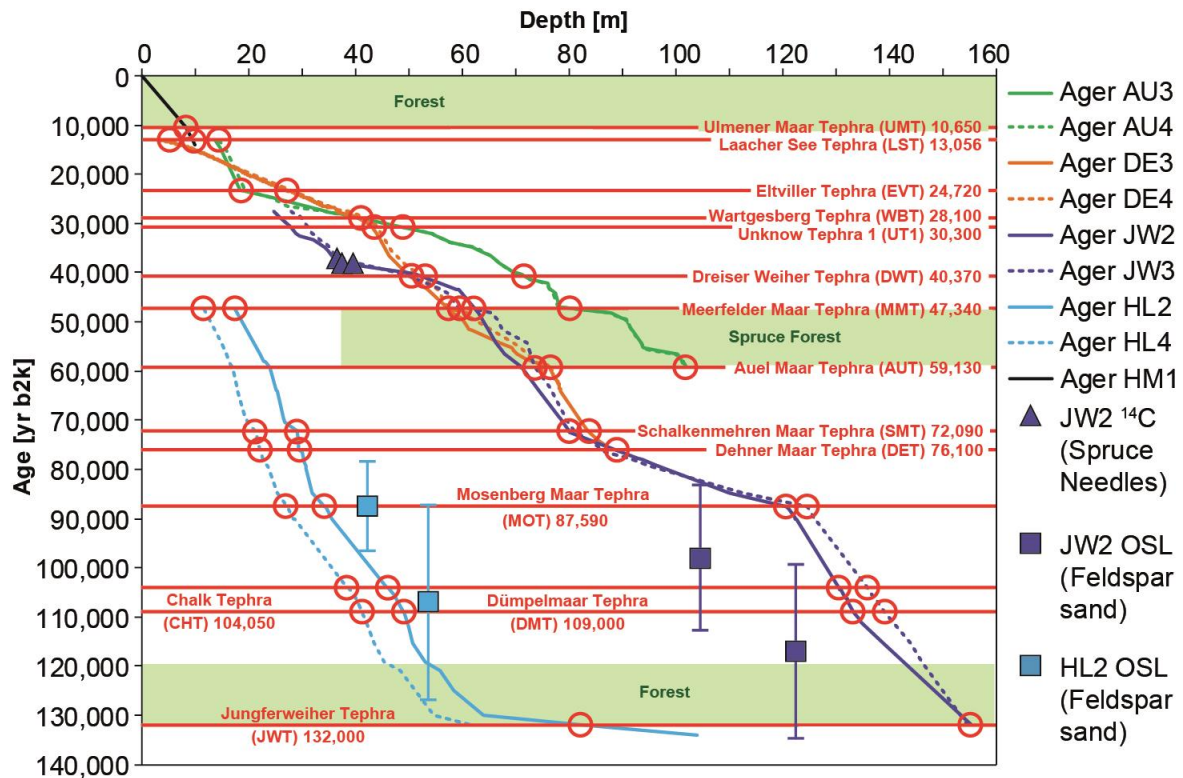
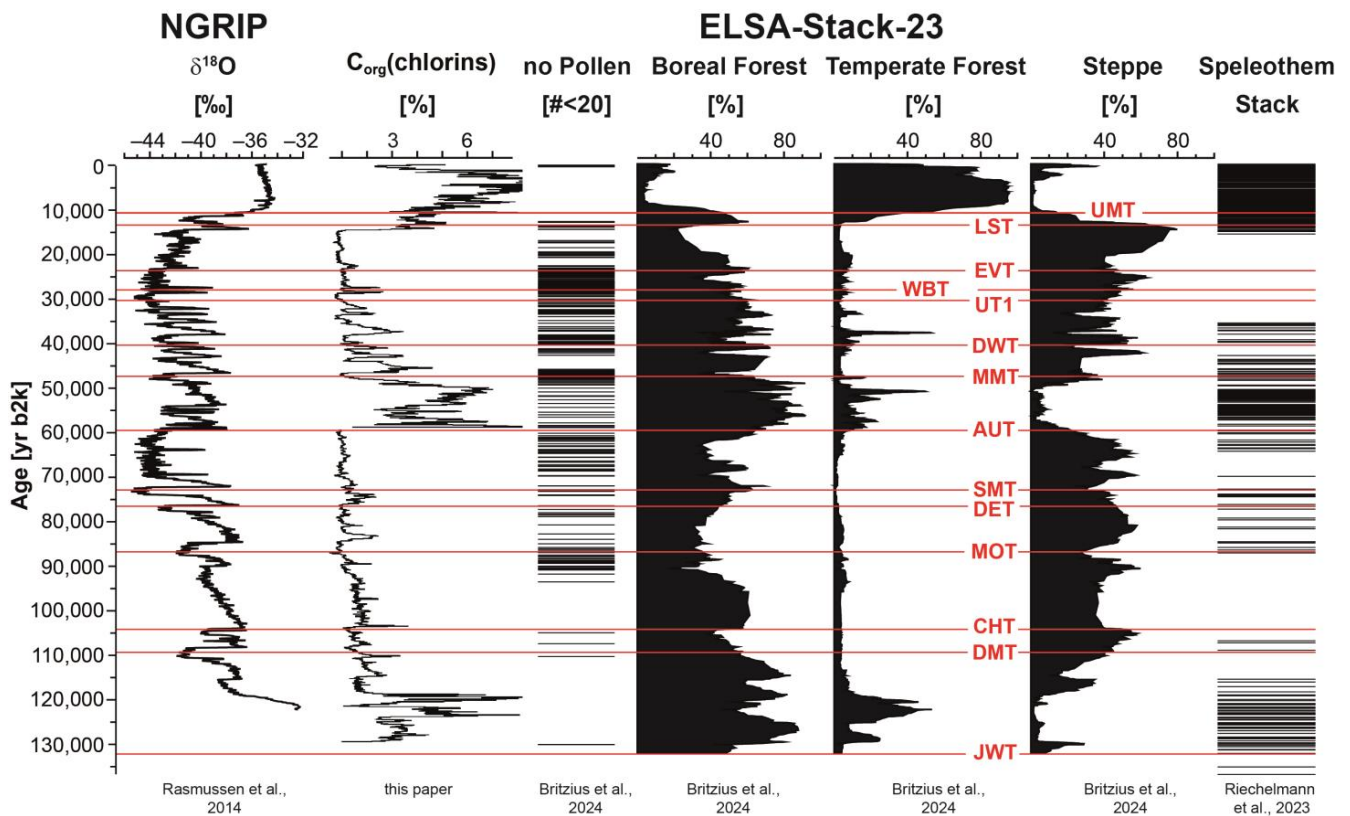
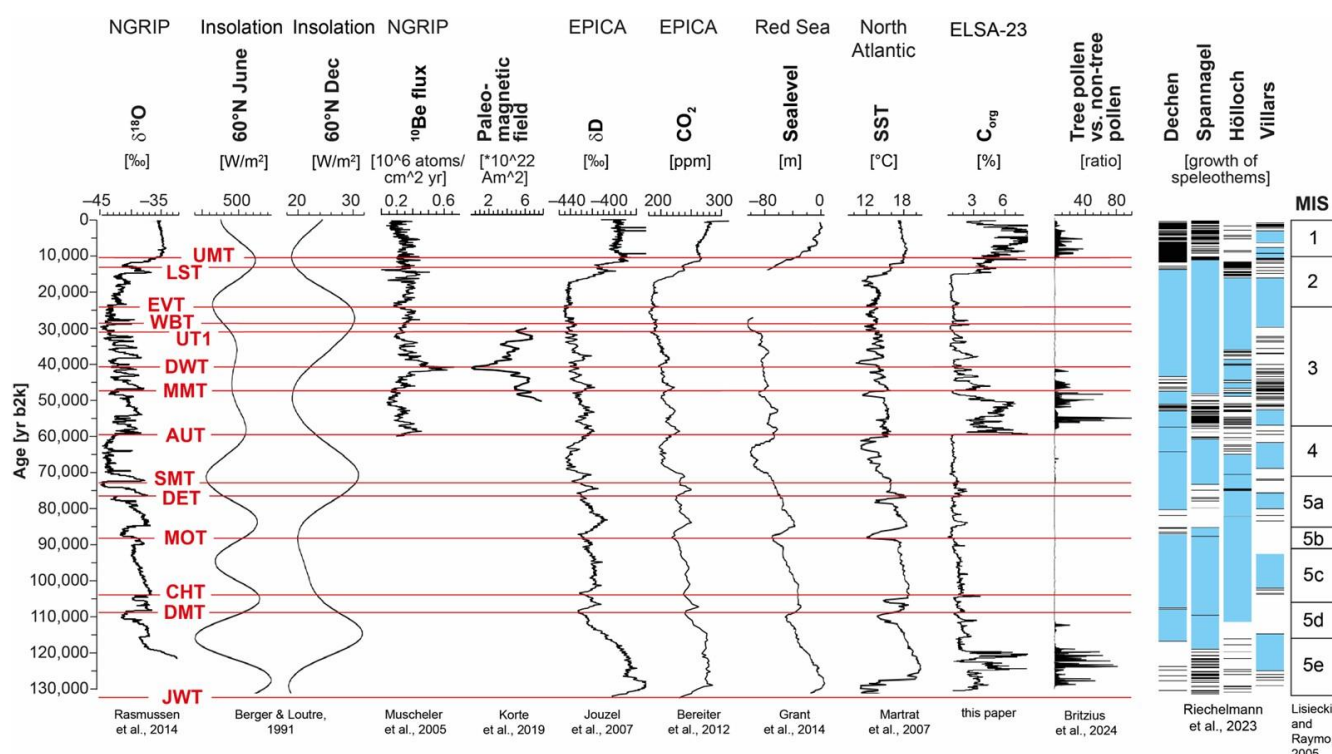


Figure 7. Age model with <sup>14</sup>C dates for the long JW2 and JW3 cores from the infilled maar of Jungferweiher (compare Figure 6). Additionally, age models of the AU3, AU4, DE3, DE4, HL2, and HL4 cores are displayed.



**Figure 8.** Synopsis of the ELSA-23-Pollen-Stack [22] (this issue) and tephra as presented in this paper (NGRIP data from [25] and speleothem stack from [26]).

Sirocko et al. [27] recently documented tight control of North Atlantic sea surface temperatures regarding the climate evolution and vegetation cover in central Europe for the last 60,000 years (Figure 9). All GIs were apparently associated with an increase in the Eifel maar lake surface water temperatures, paralleling the activity of the North Atlantic Meridional Overturning Circulation (AMOC). All interstadials witnessed the expansion of trees, at least in the Eifel, and thus most probably in many other regions of Central Europe. The millennia between interstadials were characterized by steppe-taxa, mainly grasses, as shown in the work of Britzius et al. [22] (this issue). The time series of environmental changes was recently extended by Riechelmann et al. [26], with  $C_{org}$  records back to 130,000 yr b2k, which document the synchronicity of the MIS 5 forest development and stalagmite growth phases (Figures 8 and 9). The dates of tephra were already included in the work by Riechelmann et al. [26] but are evaluated here in more detail.



**Figure 9.** Comparison of the ELSA-23 tephra with established time series of insolation [28], atmospheric CO<sub>2</sub> in Antarctic ice [29], δ<sup>18</sup>O in Greenland ice [25], variations in geomagnetic field strength [30], and solar intensity as reconstructed from <sup>10</sup>Be in Greenland ice [31]. Additionally, the δD [32], sea surface temperature [33], Marine Isotope Stages [34], sealevel changes [35], tree vs. non-tree pollen [22] and the speleothem growth from the speleothem stack [26] are displayed.

The dates for all tephra were taken from the stratigraphy of the ELSA lake sediments [9,20,27]. At first sight, Figures 8 and 9 reveal that all volcanic eruptions in the Eifel occurred very close to the times of abrupt Greenland/North Atlantic warming events. Accordingly, the Eifel volcanic activity occurred in the centuries before the North Atlantic/Greenland interstadials. Unfortunately, it is not unequivocally documented if all Greenland warming events are indeed associated with global sea-level rise. Siddall et al. [36] and Grant et al. [35] show global sea level rise before GI17, GI14, GI12, GI8, which are GIs with a length of more than 1000 years, and associated with Heinrich events before the abrupt warmings. An open question, however, is whether shorter GIs like GI4, GI3, and GI2, which lasted only a few centuries, have also been associated with sea level rise, or if they just represent changes in the North Atlantic surface water temperatures.

Sea level change is always associated with continental ice volume change, and model studies have revealed that ice volume changes affect the stress field of the continental crust [37]. In this study, we will evaluate whether the Eifel volcanic activity is indeed only related to times of sea level changes, or if they have also been affected by all GIs, and thus North Atlantic sea surface temperature changes. In this case, the AMOC would show a relationship with Eifel intraplate volcanism. Wu et al. [38], Wang and Manga [39], and Carlson et al. [40] have suggested that climate change and changes in ground water levels are indeed highly capable of changing the stress field of the continental crust because the pore space in soil sediments is filled during increases in rainwater, which adds weight to the hydrostatical pressure on a supra-regional scale. The pore space is, on average, 20% of clastic sediments, and thus an increase in the ground water level of 10 m (typical for glacial to interglacial groundwater change) results in an additional weight of 2 m water columns in areas of hundreds of square kilometers. In addition, increases in precipitation can act very locally in lakes and rivers. Bathymetric maps of modern Eifel lakes show that the

glacial terraces, i.e., the glacial lake level, are about 10–15 m below the modern lake level. Accordingly, the local hydrostatic pressure of a 10 m water column under a lake increases the weight of the continental crust above faults (always necessary for maar formation), but only locally.

In this study, we used the entire suite of ELSA lake sediment cores and their stratigraphy to document the precise temporal relationship between volcanic eruptions and the closest abrupt climate change event. Before these geodynamical topics can be evaluated further, we will first present the data basis of cores and tephra for all 14 marker tephra of the last glacial cycle.

The following chapter uses different notations for the age of the Eifel maar lakes. We present in the text the published dates with references to the respective literature. In this context, we use the age and notation as given in the original paper. The dates in this paper are presented with the ELSA-20 age notation [27], thus in [yr b2k], the official NGRIP GICC05 nomenclature.

### 1.2. The ELSA Cores

We center our focus on the 150 m long records retrieved from Jungferweiher, as they uniquely present sediment cores spanning MIS 3, MIS 4, and MIS 5 periods, with all tephra layers in superposition (Figures S1–S14). The most important tephra is the Dümpelmaar Tephra (DMT) with its unique color zonation (Figure 10). This zonation is visible in the outcrop site at Herchenberg, where it was dated  $116,000 \pm 11,000$  yr BP [17], and also in the ELSA lake sediment cores of Jungferweiher, Hoher List, and Eigelbach, where it is documented a few meters above Eemian pollen spectra (Figure 10, see also [9]). The geochemical composition was found by Sirocko et al. [20] and Förster et al. [24] to be identical to the tephra present at the Herchenberg outcrop. Its  $^{40}\text{Ar}/^{39}\text{Ar}$  date was corroborated by luminescence dating on both cores JW2 and HL2 by Degering and Krubetschek [21], who presented ages of this colorful marker tephra. A total of 20  $^{14}\text{C}$  dates of MIS 3 ages fit this age model. New dates of the core meters 34–47 m (JW2) reveal consistent radiocarbon ages of 36,300 to 39,100 cal BP, thus exactly situated in GI8 [25,41].

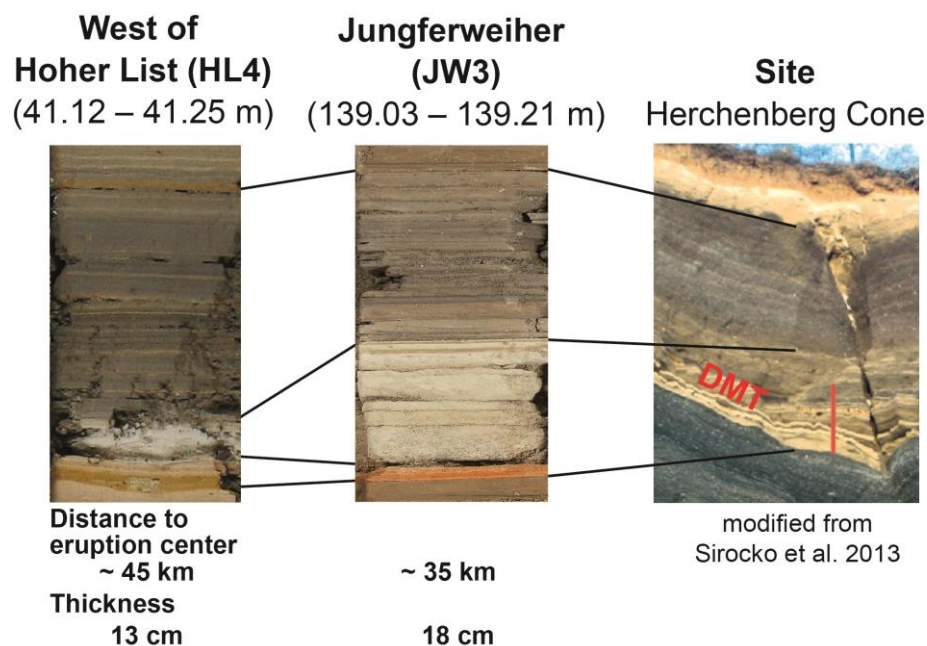


**Figure 10.** Photos of the sanidine-rich Dümpelmaar Tephra (DMT),  $^{40}\text{Ar}/^{39}\text{Ar}$  dated to  $116,000 \pm 11,000$  BP [17] at the site of eruption in the Herchenberg (EEVF) and in ELSA lake sediment cores from Hoher List and Jungferweiher [20], which can also be compared with Figure S13.

### 1.3. Tephra Layers

The thickness of tephra varies according to the distance to the eruption site and the prevailing wind direction. Accordingly, we use sediment petrography to connect some of the ash layers in the lake to potential eruption centers. For this purpose, we sampled about 50 modern tuff walls, applied the same sediment petrographic analysis as for the lake sediment tephra and included these ground data as the black column in the histograms presented in Figures S1–S14.

## 2. Methods

Photos of the entire cores used in this study have been documented in earlier studies. In this paper, we present only zoom photos into the tephra layers (Figures S1–S14). Only the core photo of JW3 is documented here as Figure 6 together with the  $^{14}\text{C}$  dates already presented by Sirocko et al. [20] (Figure 7).

### 2.1. Dating of Tephra Layers

Highly evolved tephra layers, such as the Laacher See Tephra (LST), have been dated by  $^{40}\text{Ar}/^{39}\text{Ar}$  on sanidine crystals and have an age of  $12,900 \pm 560$  BP [16], thus resulting in a very large error. However, LST deposits are also found in lake sediments throughout central Europe and are dated by varve counting to 12,880 BP [8]. The latest and most precise date for the timing of the Laacher See eruption comes from a dendrochronological study, dating the eruption to the year 13,056 yr b2k [42].

Mafic eruption centers such as scoria cones and maar volcanoes are largely devoid of primary sanidine and must be  $^{40}\text{Ar}/^{39}\text{Ar}$  dated on glass samples. Exceptionally well-preserved glasses are known from the lava flows of the Alf creek valley, which were dated to  $31,000 \pm 11,000$  BP [13]. A comparable age of  $33,600 \pm 2400$  BP has been determined for the loess below the Wartgesberg [43]. The Meerfelder Maar has been dated with  $^{14}\text{C}$  to 41,300 uncalibrated BP [44].

However, caution must be taken with respect to  $^{40}\text{Ar}/^{39}\text{Ar}$  dating of maar volcanoes in the central WEVF between Gerolstein and Daun. Their tephra deposits contain xenocrystic sanidine often also found as volcanic bombs composed of sanidinite, sourced from older intrusions of evolved magma that formed in the first stage of the volcanic field at ~500,000 yr b2k [4]. These are ages for the formation of the sanidines during their crystallization in shallow crustal reservoirs and do not represent the eruptions' dates. For example, the Dreiser Weiher Tephra (DWT) contains xenocrystic sanidine sourced from crystallized bodies of phonolitic magma that intruded into the upper crust of the central part of the WEVF during the first magmatic episode at ~500,000 yr b2k [4].

Some wood remains preserved in the tuff wall around the west Eifel maar lakes, and infilled maar lakes have been dated using  $^{14}\text{C}$  [45]. These ages have been determined by alpha spectroscopy and show ages of around 20,000 BP, but these dates are well beyond the applicability of the alpha counting used in those days and thus cannot be used to indeed date the MIS 3 tephra but have to be regarded as ages older than 20,000 BP (M. Geyh, pers. comm.).

The chronology of the tephra in this paper is based on the stratigraphy of cores AU3 and AU4 from the infilled maar lake of Auel. Both Auel cores have been analyzed with mm resolution (sub-annual) for  $\text{C}_{\text{org}}$  (chlorins), which represents the presence of chlorophyll producing algae, mainly diatoms, which flourish in this lake during times of high nutrient content and warm surface water of the MIS 3 Auel paleolake [25]. These authors also present  $^{14}\text{C}$  dates for the Auel cores by dating several different components. Most of these dates document an MIS 3 age of the Auel record, but the  $^{14}\text{C}$  record also contains wood particles, eroded from the catchment of Auel, which show ages older than the depositional age. Both AU3 and AU4 show, however, the full succession of all Greenland interstadials of MIS 3, and were thus merged into one record, the ELSA-20  $\text{C}_{\text{org}}$  stack [25].

This sub-annual resolution record was subsampled to one year resolution and tuned to the end and beginning of the MIS 3 Greenland interstadials. The ELSA-20  $\text{C}_{\text{org}}$  stack was tuned with a mathematical algorithm to the Greenland GICC05 chronology. We thus trans-

ferred the error of  $\pm 150$  years of the annual layer counted NGRIP GICC05 chronology [36], which resulted in a combined error of about  $\pm 200$  years for the ELSA-20 chronology.

The dating of the tephra in the Auel cores was performed by linear interpolation between the end and the beginning of the subsequent interstadial. We do not know if the sedimentation rate during the respective segment was indeed linear, thus adding another 50 years to the uncertainty of the tephra layers and resulting in a final age error estimate of  $\pm 250$  years relative to the GICC05 chronology. However, the error relative to the onset of the Greenland Interstadials is about 50 years, which allows us to determine the age offset of the tephra to the Greenland warming events on the scale of several decades.

The Auel based ELSA-20 chronology was then transferred to the 156 m long core JW3 from the infilled maar lake of Jungferweiher, which is used to extend the ELSA-20 chronology into MIS 5. The tuning of the MIS 5  $C_{org}$  (chlorins) maxima is not as perfect as for the Auel record, but  $C_{org}$  maxima can be related to the GICC05 ice core stratigraphy, which results in a continuous record from about 35,000 to 135,000 yr b2k. JW3 has two feldspar luminescence ages in the early MIS 5 [21] and reveals a pollen record with the typical Eemian succession at the base between 140 and 150 m. We present in this paper three new  $^{14}C$  ages from the depth assigned by the tuning to GI8; the  $^{14}C$  ages indeed exactly match the tuned age (Figure 7). AU3, AU4, JW3, and also the cores HL2 and HL4 from the infilled maar of the Hoher List show the same succession of distinct tephra layers, which are mineralogically and geochemically correlated between all five cores. These present together the basis of the ELSA-23 chronology, which now covers the entire time span from today to 132,000 yr b2k (Figure 8).

## 2.2. Petrography of Tephra Layers

Tephra from maar lakes, scoria cones, and evolved volcanoes (Figures 3–5) are distinguishable by their content of mafic minerals (pyroxene), white minerals that are indicative of evolved lavas (leucite, sanidine), rock fragments (reddish and grayish sandstone, quartzites), and scoria and pumice/glass. Maar tephra, in contrast, are rich in fragments of country rock that are composed of reddish and grayish sandstones in the Eifel region (Figures 11 and 12). Förster and Sirocko [23] developed a method to distinguish the lake sediment tephra by counting certain minerals/components and presented the results as a histogram, which we present here for all 14 marker tephra in Figures S1–S14. The potential samples for marker tephra were recently re-evaluated and counted again, including additional samples. These were analyzed with a reduced list of minerals/components (reddish sandstone, grayish sandstone, amphibole, pyroxene, scoria and mica) in comparison to the work of Förster and Sirocko [23]. Quartz, pumice, and leucite were removed from the new counting procedure, although pumice and leucite will continue to be mentioned separately if they are of characteristic importance to a tephra (Figure 12). The quartz content from a single tephra can show a wide range of values, depending on the core from which it was sampled. This is likely due to quartz being transported by the eruption itself if a quartz vein was present in the ejected strata or transported as non-volcanic sediment into the maar lake by either eolian and/or fluvial transport during the eruption of the corresponding tephra. Pumice was excluded since it is difficult to handle during sieving ascribed to its buoyant behavior leading to potential skewed results. During the re-evaluation, it was found that leucite, if present, was found only in the initial layers of tephra. Therefore, leucite does not have to appear in all tephra deposits of a corresponding eruption across the sampled maar lakes, probably because of changing wind directions during the eruption.

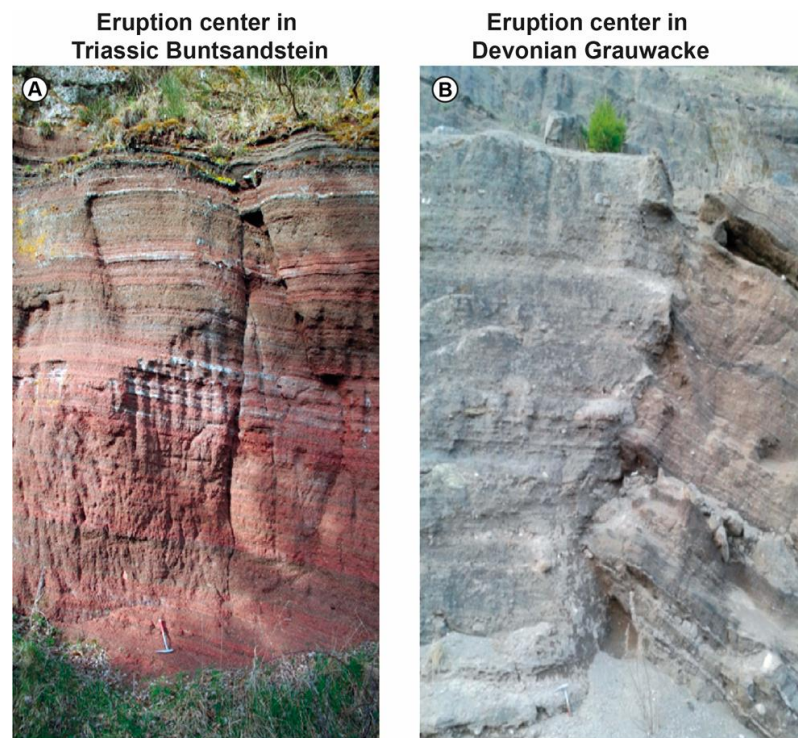


**Figure 11.** Photos of the tuff wall for two maar eruptions, including (A) one eruption that occurred in a region of reddish Buntsandstein rocks; (B) the other that occurred in a region of grayish Devonian Grauwacke.



**Figure 12.** Sediment petrography of the fraction 150–250 μm used to classify the volcanic ash layers in the ELSA lake sediments. Original photos from ELSA sediment cores. Grayish and reddish sandstone represent fragments from the surface rocks at the site of eruption. Pyroxenes characterize mafic eruptions and while sanidines characterize highly evolved magma or xenocrystals from evolved crustal reservoirs.

### 2.3. Geochemical Characterization of Tephra Layers in the Lake Sediments

Glasses from widespread and young evolved tephra layers from the East Eifel Volcanic Field (EEVF), such as the LST, have been geochemically identified within ELSA maar drill cores before [20]. However, for the basaltic maar and scoria cone volcanoes, the glass samples are low in  $\text{SiO}_2$  and are more prone to alteration, and thus show changes in alkaline and earth alkaline metal content. For the basaltic volcanoes, we performed 2200 clinopyroxene analyses at 16 sites [24]. The source volcanoes belong to the three different magma suites of 'foiiditite' (F)-, 'olivine nephelinite and basanite' (ONB)-, in the West Eifel, and 'basanite east' (BE)-suite in the East Eifel [3], which enabled us to distinguish between individual tephra layers by their clinopyroxene chemistry. In Figure 13, we present the analyses of the glass and clinopyroxenes of the selected tephra that reveal a distinct fingerprint in the geochemical composition. While glass samples of mafic tephra are widely scattered (Figure 13A) and the glass fragments of the highly differentiated DMT are less altered and located within the field of young (<215 ka) plagioclase phonolite-trachyte composition of the EEVF, showing distinctly high  $\text{SiO}_2$  of >60 wt.%. Mafic tephra are best compared by their clinopyroxene geochemistry (B) of the Al(VI) vs. Al(IV) relationship, which shows distinct groups depending on the clinopyroxene crystallization depth. The eruption sites and their corresponding tephra ages in the ELSA lake sediments were as follows (Figure 13B): LST was associated with Auel core AU2 at 13.90 m. The Eltville Tephra (EVT) from the Remagen location (REM3A 4.40 m) and samples of Auel core AU3 at 24.40 m correlate with clinopyroxenes from the young BE-suite scoria cone Wingertsberg. The Wartgesberg Tephra (WBT) corresponds with AU2 at 36.80 m and Dehner Maar core DE3 at 37.90 m. The Schalkenmehrener Maar Tephra (SMT) aligns with JW3 at 80.90 m. The Mosenberg Tephra (MOT) connects with HL4 at 27.30 m and JW3 at 124.60 m. The Jungferweiher Tephra (JWT) corresponds with JW3 at 154.40 m and HL2 at 82.20 m (see also Figure 7).

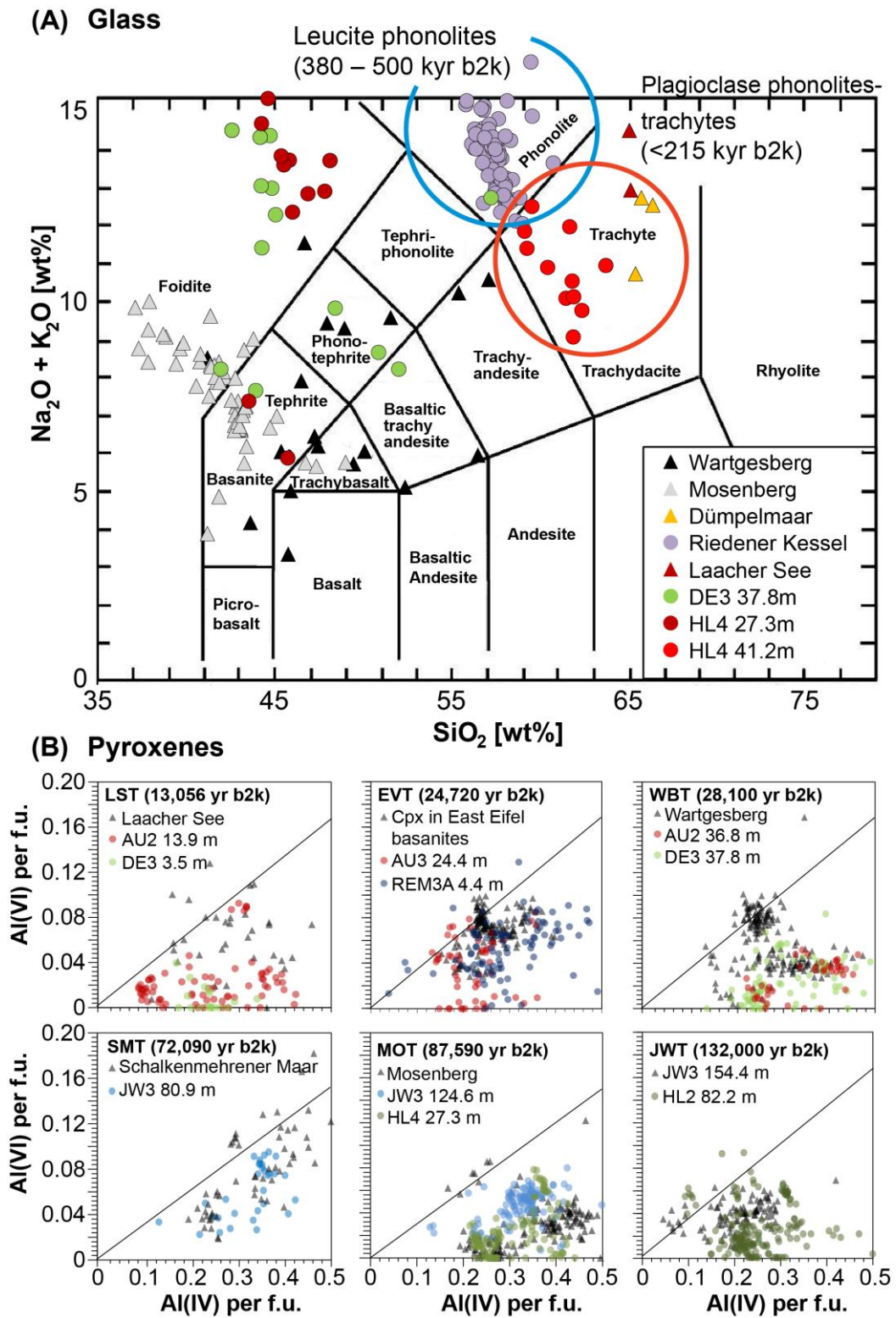


**Figure 13.** Geochemical fingerprint for selected tephra (modified from Förster et al. [24]). Glass samples of mafic tephra are widely scattered (A), while the glass fragments of the highly differentiated Dümpelmaar Tephra are less altered and located within the field of young (<215 ka) plagioclase phonolite-trachyte composition of the EEVE, showing distinctly high SiO<sub>2</sub> of >60 wt.%. Mafic tephra are best compared by their clinopyroxene geochemistry (B) of the Al(VI) vs. Al(IV) relationship that show distinct groups depending on the clinopyroxene crystallization depth.

### 3. Results: Documentation of the 14 Marker Tephra Layers Deposited in the Maar Lake Sediments of the Last 130,000 Years

#### 3.1. Ulmener Maar Tephra (UMT) 10,650 yr b2k (Figure S1)

An overview of the 14 marker tephra of the last 130,000 years starts with the Ulmener Maar Tephra (UMT), which is the youngest volcanic eruption of the Eifel Volcanic Fields. It was dated to 10,000 BP using wood residuals [45]. Varve counting of the UMT in the first Holzmaar records resulted in an age of 11,000 varve years BP [7]. Varve counts in lake sediments from the Meerfelder Maar place the UMT at 11,200 varve years BP [8].

The UMT is well documented in ELSA core HM1 from Holzmaar as a 3 mm thick layer at 8.5 m (Figure S1). An ELSA varve age for this tephra will be provided with the upcoming ELSA varve stack. For  $^{14}\text{C}$  dating of the Ulmener Maar eruption, we collected 12  $^{14}\text{C}$  samples in a tunnel through the Ulmener Maar tuff wall. Three samples from the roots of a standing tree, which grew at the site during the time of eruption, gave consistent ages of 11,107 to 10,575 yr cal BP, which we used to calculate the eruption age as 10,650 yr b2k. The 12  $^{14}\text{C}$  samples of wood/roots were analyzed at the CEZA laboratory in Mannheim.

#### 3.2. Laacher See Tephra (LST) 13,056 Dendro Year b2k (Figure S2)

The Laacher See is the youngest eruption center of the EEVF. Its cataclysmic eruption dwarfs all other volcanic eruptions of both Eifel Volcanic Fields [5,46]. The tephra layer is widespread across Europe and appears in lake sediments as far as Finland and Switzerland. The visible layers in the lake sediments do not always represent air fall but show colors from the rocks of the surrounding geological strata. Apparently, the LST at Auel has a reddish color because most of the particles were washed into the lake from the catchment with outcrops of reddish Devonian or Triassic sandstones (Figure S2). The LST is always associated with abundant pumice and sanidine, which can reach more than 40% of particles. The geochemistry of pyroxenes from the lake sediments reveals an identical composition of pyroxenes at the eruption site (Figure 13). Typical minerals of the LST such as hauyn are not observed in the lake sediments because this mineral is unstable under oxic conditions in lake water.

#### 3.3. Eltville Tephra (EVT), 24,720 yr b2k (Figure S3)

Numerous loess deposits of the Last Glacial Maximum show a widespread tephra layer in the Netherlands, Belgium, and Southwest Germany. The origin is likely from the EEVF [24,47]. A compilation of ages in loess deposits yield an age of  $24,300 \pm 1800$  yr b2k [48]. The tephra contains mainly mafic minerals, such as clinopyroxene, amphibole, and scoria. It appears in the varve-counted DE3 record at 30.57 m as a 2 mm thick dark layer of tephra at 24,720 yr b2k, i.e., 3.41 m before the onset of GI2, which is dated to 23,340 yr b2k [36] (Figure S3). The glacial sediments of Auel do not allow a precise age determination for this interval, but the tephra at 24.41 m is immediately before a small sulfur spike, which we attribute to GI2.

We conducted an electron microprobe analysis to compare the geochemistry of the EVT in AU4 and DE3 with samples from the Remagen EVT (kindly provided by P. Fischer, Mainz). The geochemistry points towards a source from the EEVF. Further discussion of the EVT source regions and their respective geochemical data for all other tephra were presented by Förster et al. [24].

#### 3.4. Wartgesberg Tephra (WBT) 28,100 yr b2k (Figure S4)

The Wartgesberg is the largest scoria cone complex of the WEVF (Figure 4) and was dated previously to  $31,000 \pm 11,000$  BP [13],  $33,600 \pm 2400$  BP [43], and 32,000–25,000 BP [49]. The volcano consists of several amalgamated scoria cones and two large lava flows extending from 2 to 6 km from the complex (Figure 4). The ELSA drill-cores show three 10–30 cm thick mafic tephra layers between GI3 and GI4 (28,100 yr b2k) that correlate in petrographic composition and time with the Wartgesberg complex (Figure S4). The main tephra is thus

accompanied by two smaller tephra, which show a similar mafic composition to the main eruption but are more enriched in rock fragments from phreatomagmatic activity and thus document contributions from nearby maar structures, most likely the Sprinker Maar and Trautzberger Maar. The tephra occurred 320 years before the onset of GI3 and 500 years after GI4.

### 3.5. Unknown Tephra 1 (UT1) 30,300 yr b2k (Figure S5)

A similar mafic tephra layer is also present at 30,300 yr b2k and shows a composition similar to that of the WBT, with higher contents of country rock fragments (Figure S5). It may be an earlier eruption of the Wartgesberg complex or another mixed maar–scoria cone eruption in the South-East of the West Eifel, potentially the Holzmaar, whose time of eruption has not been precisely identified yet, but must be older than 27,000 varve years BP [8]. Unfortunately, Holzmaar has no tuff wall, and thus, the mineral composition of the eruption cannot be determined. UT1 occurred between GI5 and GI4 at 30,300 yr b2k, which places the eruption at the beginning of the H2. Another possible eruption center of a mixed phreatomagmatic and scoria cone eruption is the Booser Doppelmaar complex.

### 3.6. Dreiser Weiher Tephra (DWT) 40,370 yr b2k (Figure S6)

The Dreiser Weiher is located within the center of the WEVF. Given its phreatomagmatic origin, the DWT consists largely of country rock fragments of grayish and reddish sandstone, and pyroxenes (Figure S6). In addition, the tephra contains xenocrystic sanidine, which is sourced from older intrusions of phonolitic magma within the central part of the WEVF [4]. The tuff wall of the Dreiser Weiher is well known for its large olivine bombs. Olivine is, however, not stable in the lake sediments and was never observed in any maar lake layer of the DWT. The DWT is dated about 100 years before GI9, thus at an age of 40,370 yr b2k. We carefully checked the DWT for greenish pyroxenes and twisted minerals, as found in the Campanian Ignimbrite (CI) [50] (this issue), but these minerals were not found in the DWT.

### 3.7. Meerfelder Maar Tephra (MMT) 47,340 yr b2k (Figure S7)

The Meerfelder Maar is a large maar volcano in the South-East of the WEVF. The tephra layer is rich in country rock of reddish and grayish sandstone (Figure S7). The Meerfelder Maar was dated previously by  $^{14}\text{C}$  with an uncalibrated age of 41,300  $^{14}\text{C}$  BP [44]. The age of the MMT in the ELSA-20 chronology is at 47,340 yr b2k, which places it to the end of H5, shortly before the onset of GI12.

### 3.8. Auel Maar Tephra (AUT) 59,130 yr b2k (Figure S8)

The ELSA-20  $\text{C}_{\text{org}}$  time series ends at 59,130 yr b2k with the eruption of the Auel maar [25]. The site of Auel is only a 2 km distance to the Dehner Maar and accordingly, we observed a thick tephra of 80 cm thickness in the Dehner core DE3 (Figure S8). The Auel tephra was not sampled from the Auel tuff wall because this is not clearly distinguishable in the landscape, but at the base of core AU2, which was drilled 10 m into the late eruption fallout. The Auel tephra is characterized by a high content of reddish sandstone fragments derived from nearby Buntsandstein outcrops or reddish Devonian sandstones, which are also exposed in the catchment of the Auel maar site. Sirocko et al. [25] determined an age of 59,130 yr b2k in the tuned lake sediment records of cores AU3 and AU4.

The record of AU2, however, is deeper than AU3 and AU4, and we realized that the Auel Maar Tephra (AUT) already becomes visible before a  $\text{C}_{\text{org}}$  (chlorins) peak, which could represent GI18. If this possible connection is considered, the AUT could have an age of about 64,000 yr b2k. The final age determination for the AUT is still open but will be derived by the ongoing varve counts of core DE3 (Sirocko, unpublished).

### 3.9. Schalkenmehrener Maar Tephra (SMT) 72,090 yr b2k (Figure S9)

Apart from displaying a high content in grayish sandstone, the appearance of leucite distinguishes the SMT from most other maar tephra layers. Leucite minerals have been reported from the tuff wall of the Schalkenmehrener Maar [3,4] where we sampled it, but leucites were weathered to analcime [23]. Not all of the samples attributed to the SMT indeed contain leucite. This could be explained by the weathering of leucites in soils and lake sediments, as well as by changes in wind direction. The high amount of leucites in the Jungferweiher core JW3 at 80.94 m, 5 km east of Schalkenmehren, indicates a prevailing wind direction from the west. It is possible that the wind that transported the SMT towards the NW to the Dehner Maar was blowing only in the later phase of the eruption. If the leucite was concentrated in the initial eruption cloud, it would explain why this mineral was not found in the SMT layer at the Dehner Maar and Auel Maar. The SMT appears in the cores HL2 and HL4 as a thick layer containing chunks of ejected strata as well as scoria, which show signs of welding. Geochemical investigations of clinopyroxenes by means EPMA show that samples from the Schalkenmehrener Maar plot were among those found in JW3 at 80.9 m (Figure 13B). Detailed plots of Al(VI) versus Al(IV) and Ca/Na versus Mg# indicate that the Schalkenmehrener Maar clinopyroxenes crystallized in the lower to middle crust from mafic to intermediate melts (Figure 13B).

### 3.10. Dehner Maar Tephra (DET) 76,100 yr b2k (Figure S10)

The oldest tephra in the DE3 core is from the Dehner Maar itself and appears at 79.61 m depth (Figure S10). The DET is, together with the SMT, the most important tephra to synchronize the MIS 3 lakes with the older MIS 5 lakes. We find a 5 cm tephra layer of similar composition in the cores JW3, DE3, HL2, and HL4 (Figure S10).

The age of the DET is slightly older than that of the SMT, but still younger than that of GI21, which is clearly visible in all four cores (Figure 14). The difficulty for comparison comes from the peculiar position at the very top of the HL cores and at the very base of the DE cores. It is thus the position in the continuous JW3 record that we use for the final age determination after GI21 and before GI20, with an approximate age of 76,100 yr b2k.

### 3.11. Mosenberg Tephra (MOT) 87,590 yr b2k (Figure S11)

This colorful tephra of about 10 cm thickness is visible in all cores of this time interval (Figure S11). The annual layer counts in core HL2 reach close to this tephra and gave an age of about 80,000 varve yr BP [9]. This date corresponds very closely to the luminescence dating reported by Zöller and Blanchard [51], who also measured 80,000 BP on slate xenoliths from the Mosenberg outcrop. Geochemical investigations on pyroxenes by Förster et al. [24] support this assignment in the field and the cores. However, the fine striations in two cores (JW3 and HL4) show that this eruption occurred in several phases, or that contemporary eruptions took place at other locations that led to a complex tephra composition. The tuning of the HL4  $C_{org}$  (chlorins) curve to the Greenland ice places the MOT at an age of 87,590 yr b2k.

### 3.12. Chalk Tephra (CHT—Former Unknown Tephra 5 (UT5))—104,050 yr b2k (Figure S12)

The Chalk Tephra (CHT/UT5) is characterized by 50% pyroxenes but also contains about 30% grayish sandstone fragments (Figure S12). This is neither the composition of a typical maar tephra nor of a pure strombolian eruption. The most likely explanation is an initial phreatomagmatic maar eruption that subsequently led to a magmatic eruption. During the course of the ELSA drillings, we found three locations that are morphologically clearly a maar but filled with volcanic cinders up to a drilling depth of 30 m. These are the Duppacher Maar, the Kirchweiler Maar, and the Gerolsteiner Maar. In Duppach and Gerolstein, the slags originate from a cinder cone that is still clearly visible in the terrain immediately adjacent to the maars; in Gerolstein, however, an associated basalt flow has been dated to about 30,000 years ago with  $^{40}\text{Ar}/^{39}\text{Ar}$  [13]. Although, it is quite possible that this lava flow is younger than the Gerolsteiner Maar. Finally, Kirchweiler, Duppach,

and Gerolstein are still candidates to represent the site of eruption for the CHT (formerly called UT5 by Förster and Sirocko) [23].

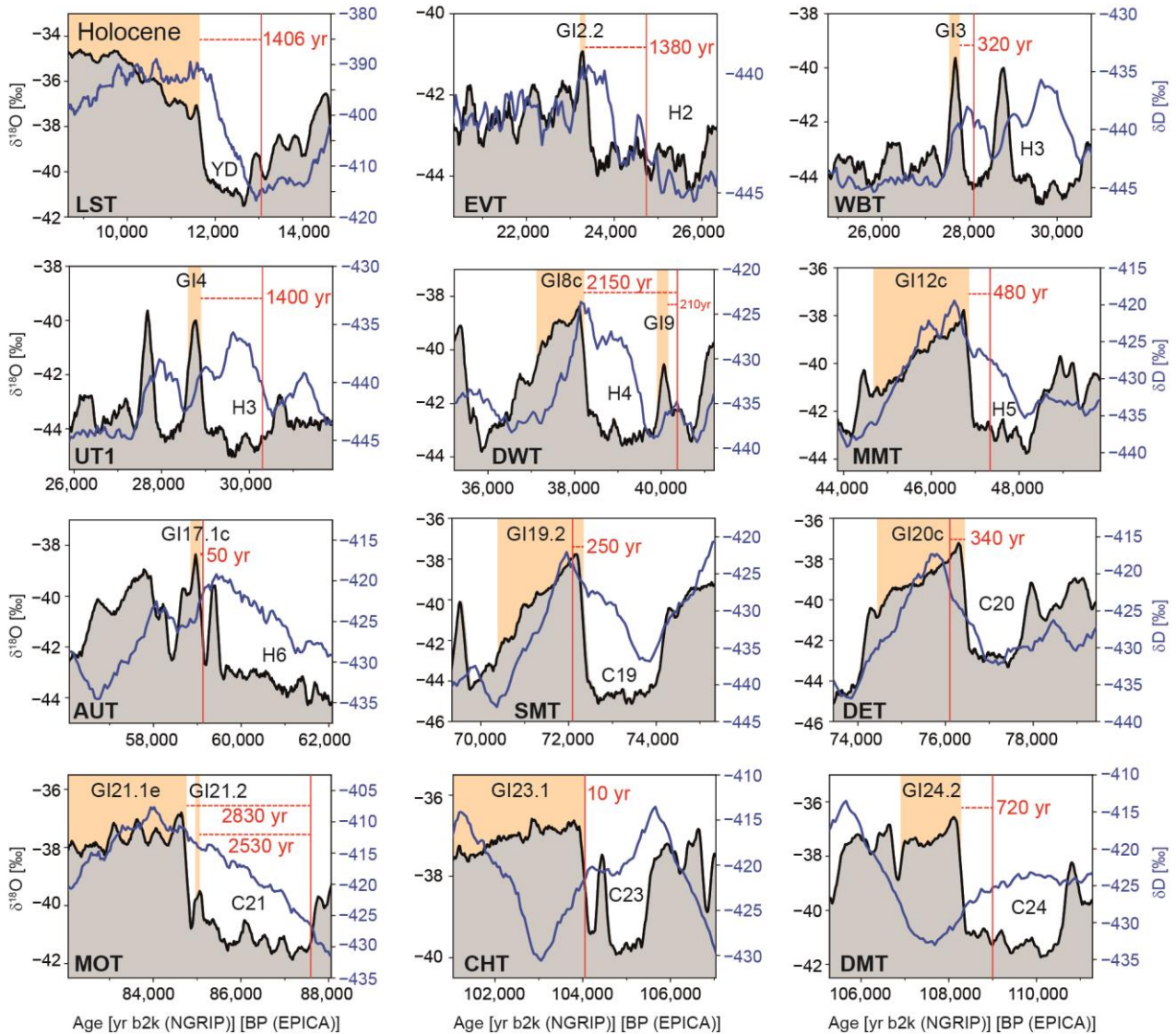


**Figure 14.** Temporal relation of the ELSA-23 tephra to the nearest warming event, with EPICA  $\delta D$  shown in blue [39] and NGRIP  $\delta^{18}O$  shown in black [36]. Time scale taken from the original publications.

We used a unique feature of this tephra layer to name it Chalk Tephra; indeed, the tephra in all cores apparently contains carbonates and inspection with a binocular reveals these carbonates as lake chalk. Chalk forms only under warm climate conditions and this eruption occurred during an interstadial, i.e., the beginning of GI23 according to its position in the  $C_{org}$  record of Jungferweiher and Hoher List cores (Figure 9).

### 3.13. Dümpelmaar Tephra (DMT) 109,000 yr b2k (Figure S13)

This colorful striking maar tephra is found in four cores and is probably the best recognizable marker tephra of the entire West Eifel (Figures 13 and S13). The tephra originates from the East Eifel, i.e., from about 50 km away and its fallout must have covered the entire West Eifel; respective photos were already reported by Sirocko et al. [20]. The typical color zonation is found in the East Eifel in the Herchenberg outcrop and the sanidine minerals common in this highly differentiated tephra are dated at Herchenberg to

116,000 ± 11,000 years by van den Bogaard et al. [17]. It was also dated by varve counting to 106,000 yr by the first annual layer counting in core HL2 [9], which is within the error range of the original  $^{40}\text{Ar}/^{39}\text{Ar}$  dating. Its position in the HL4 and JW3  $C_{\text{org}}$  records is exactly at the onset of GI24, with an ELSA-23 age of 109,000 yr b2k on the GICC05 scale.

### 3.14. Jungferweiher Tephra (JWT) 132,000 yr b2k (Figure S14)

Shortly below the first warm-period pollen of the last interglacial period (in terrestrial Quaternary geology called Eemian), corresponding in principle to MIS 5e, a tephra is found in the varve counted core HL2, but also in the basal fallout from JW3 at 155 m (Figures 6 and S14). The modern Jungferweiher is very large but has no tuff wall. It is likely that the tuff wall has collapsed into the deep crater depression of the initial maar basin. Accordingly, we sampled the tephra at the base of JW3 to document the typical mineral composition of this maar eruption. A specific feature of the JWT is whitish, strongly weathered sandstone, which can also be found in the outcrops on the southwestern flank of the maar structure. The JW3 core provides a complete pollen spectrum for the Eemian [9] and the time of eruption must be well before the onset of the Eemian. Thus, we assign an eruption age of about 132,000 yr b2k for this largest maar of the Eifel.

Figure 15 summarizes the succession of all 14 marker tephra presented in this paper and the age covered by the respective ELSA sediment cores. The JWT is the most important marker layer for extending the ELSA tephra time series even further back in time, as it is also observed in the uppermost sediments of core WD1 from Walsdorf, which we will present in the near future to extend the ELSA-Tephra-Stack back to the begin of MIS 7 (Figure 15). WD1 is dated with luminescence analyses [21] and shows a high number of tephra layers, including the  $^{40}\text{Ar}/^{39}\text{Ar}$  dated Gleys Tephra (GLT) (151,000 yr b2k) and Hüttenberg Tephra (HBT) (215,000 yr b2k).

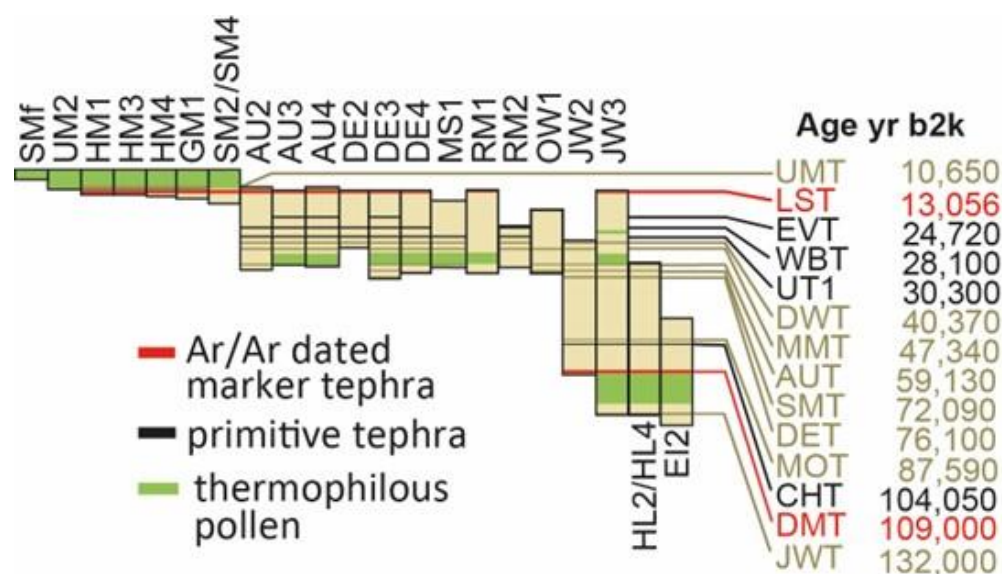


**Figure 15.** Overview of the Tephra in ELSA cores with ages determined from the ELSA-23 chronology.

Other tephra that were used by Förster and Sirocko [23] are not included in this paper. These are Unknown Tephra 3 (UT3) that were not found in all cores presented in this paper, and GLT and HBT, because they are beyond the temporal focus of this paper. Furthermore, four new tephra were added: EVT, AUT, MOT, and CHT. The MMT and SMT were formerly named UT2 and LcT, respectively.

## 4. Discussion

Table 1 presents only the marker tephra, which we observed in several sediment cores from the Eifel maar lakes of a certain period. Accordingly, the durations of the maar

eruptions must have been long enough to have been affected by changing wind directions and the spread of tephra over the entire region. Small local eruptions of short durations may form individual tephra layers in a single lake. However, they cannot be regarded as marker tephra and have not been documented in the ELSA-23-Tephra-Stack. Accordingly, our 14 marker tephra do not represent the entire number of volcanic eruptions during the last glacial cycle, but only the most prominent, well-visible events.

**Table 1.** Ages and depths of all tephra of the ELSA-23-Tephra-Stack in all dated ELSA lake sediment records (\* the UMT does not qualify as a marker tephra in this paper but is important nonetheless, as it is the youngest of the known Eifel tephra). We discuss the limitation of the age error calculations in Section 2. The age error for the tephra of the last 60,000 years should be about  $\pm 250$  years and the age error for the MIS 5 section could be even larger.

Tephra	Age [yr b2k]	HM1	AU3	AU4	DE3	DE4	HL2	HL4	JW2	JW3
		Depth [m]								
UMT * top	10,650	8.480								
UMT * base		8.485								
LST top	13,056	9.540	13.590	14.400	3.400	5.270				
LST base		9.580	13.690	14.500	3.475	5.330				
EVT top	24,720		24.360	24.150	30.480					
EVT base			24.440	24.160	30.570					
WBT top	28,100		36.800	36.830	37.799	39.820				
WBT base			37.020	36.890	37.920	39.910				
UT1 top	30,300		46.550		42.760	43.520				
UT1 base			46.680		42.910	43.650				
DWT top	40,370		71.110	70.910		54.540			51.360	49.160
DWT base			71.160	70.930		54.565			51.530	49.250
MMT top	47,340		81.740	81.150	57.580	59.540	17.510	11.610		62.480
MMT base			81.780	81.170	57.630	59.560	17.520	11.620		62.500
AUT top	59,130			102.380	76.240					73.940
AUT base					76.370					73.950
SMT top	72,090				83.400		27.100	20.210	79.690	80.800
SMT base					83.560		28.990	21.200	79.970	80.940
DET top	76,100				87.000		29.410	22.190		86.270
DET base					88.000		29.420	22.210		86.280
MOT top	87,590						34.260	27.260	120.500	124.660
MOT base							34.310	27.300	120.830	124.680
CHT top	104,050						46.000	38.410	130.270	135.740
CHT base							46.130	38.520	130.620	135.850
DMT top	109,000						48.830	41.180	133.170	139.030
DMT base							48.990	41.230	133.410	139.210
JWT top	132,000						82.000			154.850
JWT base							83.000			155.000

Several of these marker tephra may represent more than one eruption site because it is quite likely that several maar eruptions occurred at exactly the same time. Tephra with prominent zonation, such as DWT, MOT, or DMT, could be candidates for multiple synchronous eruptions. This would also explain why a zonation is not necessarily visible in all records, depending on the wind direction of each single eruption. Some of the observations of color/mineral change within a tephra layer do not necessarily show a change in the ejecta composition of one eruption but can show separate, synchronous eruption events. Such a structure is not only difficult for petrographic characterization but also leads to inconsistent patterns in the petrographic histograms. Accordingly, for our discussion on the origin of the Eifel volcanism, we will only use these marker tephra, which are consistent

between different sites and can be accurately dated in comparison to the climate-driven  $C_{org}$  records that we use to transfer the GICC05 scale to the ELSA maar records.

#### *Relation between Phreatomagmatic Maar Eruptions and North Atlantic Heinrich Events*

Most tephra layers occur before the warming events of the Northern Hemisphere interstadials. Indeed, all MIS 3 Heinrich events and MIS 4/5 C-events were associated with phreatomagmatic maar eruptions in the Eifel (Figure 9), i.e., active volcanism occurred over the Eifel mantle plume, which indicates a relationship between ice sheet decay, global sea level change, asthenospheric processes, and volcanic activity (Figure 16). Heinrich events are the Northern Hemisphere response to Southern Hemisphere warming (visible in the EPICA  $\delta D$  record), paralleled by  $CO_2$  increase [35], and probably (within the dating error) causing global sea level rise [28]. Figure 17 presents a comparison of the Antarctic and Greenland temperatures, global atmospheric  $CO_2$  increase, global sea level rise, and Northern Hemispheric Heinrich events, which appear to be the boundary conditions of the maar eruptions in the Eifel volcanic fields of central Europe. The close temporal relationship of volcanic activity in the Eifel with global climate change can be explained by the following two alternative scenarios of atmosphere–mantle connection:

1. Primary changes in the upper mantle may cause changes in the heat flow trapped under continental ice sheets. If ice sheets are thick enough to be near the point of basal melt, they will surge as soon as the threshold for basal melt is reached. An alternative endogenic–exogenic forcing could imply intensification of Mid-Ocean Ridge spreading rates, warming of ocean water, and increase in water volume, leading to sea level rise, which destabilized the shelf-based ice proportions, leading to a surge in continental ice.
2. The other scenario is exogenic forcing, which causes an endogenic response. If ice sheets increase and decrease in size by climatic forces only (insolation, ocean currents, greenhouse gases), one must assume that the changes in the lithospheric stress and associated changes in the oceanic crust stress field are due to the increase in water mass in the oceans and/or loss of ice on the continents (Figure 16). These changes in the global lithospheric stress field could activate tectonic faults that connect the Earth's atmosphere and surface to the mantle/asthenosphere during times of isostatic adjustment. Under this scenario, exogenic climate forces would act as a trigger for tectonic activity and volcanism.

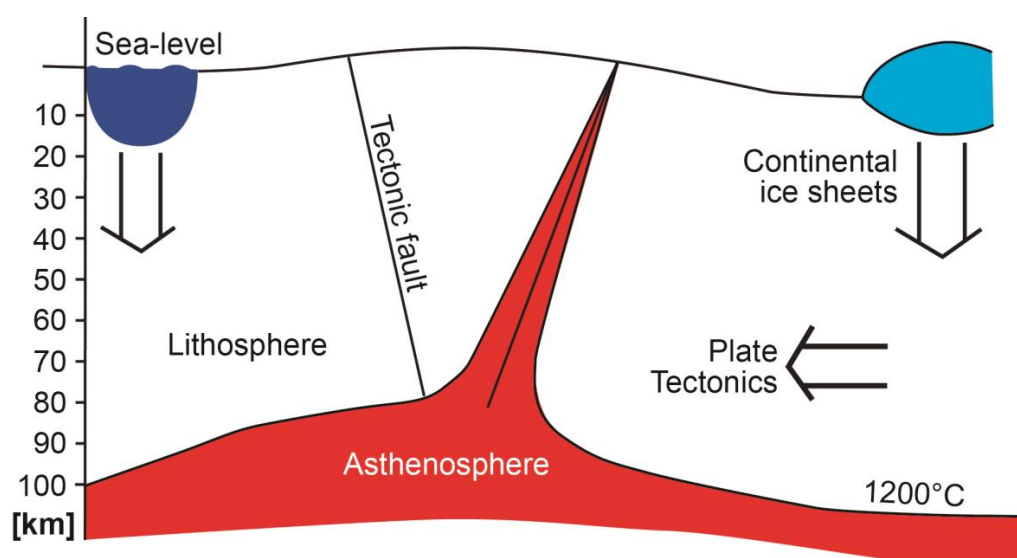


**Figure 16.** Schematic sketch of the potential endogenic and exogenic processes causing mantle plume rising, uplift and finally a maar/volcanic eruption in the uplifted regions.

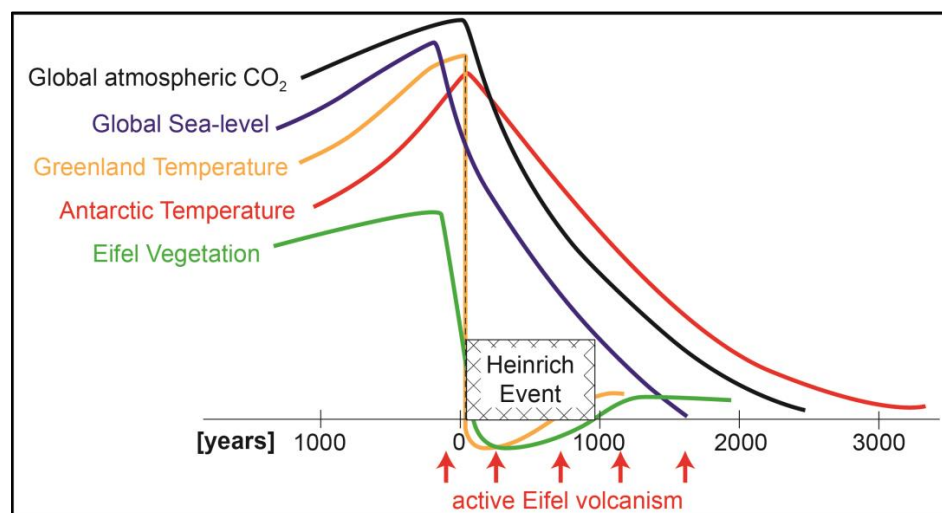


**Figure 17.** Temporal relationship between active Eifel volcanism and warming phases.

The data from the Eifel ELSA cores do not provide a clear indication for one or the other explanation. However, the synchronicity between these endogenic and exogenic processes clearly suggests that the Earth and atmosphere are indeed a coupled system, especially during times of abrupt climate change.

## 5. Conclusions

1. The Eifel volcanism during the last glacial cycle is characterized by 14 tephra layers from volcanic eruptions, which are visible in all cores across the entire Eifel.
2. The eruptions must have taken place over several days to weeks, which are necessary to explain the regional extent of these marker tephra.
3. Some of the tephra were connected to an eruption site by studying the sediment petrography of the tuff wall around the maar structures and comparing them with discrete tephra layers in the ELSA sediment cores.
4. Tephra from phreatomagmatic eruptions can be best differentiated from volcanic ashes by the amount of host rock fragments, which are derived from the Devonian and Triassic rocks at the site of eruption.
5. Most marker tephra occurred during cold phases (Heinrich events and C-events), when the continental ice sheets decayed, meaning they are synchronous with global sea level rise and synchronous with the loss of ice-load on the continents.
6. Several tephra have occurred during warm phases; however, they always occur in close connection to times of abrupt warming when precipitation over land has increased, leading to local lake level rise or regional soil moisture change.
7. Color changes and associated changes in mineral compositions indicate that several of the tephra represent multiple, synchronous eruptions from maar volcanoes and scoria cones.
8. The focus of eruptions in the millennium before warming can be explained by a relationship between Eifel intraplate volcanism and global sea level and Scandinavian ice load, which have the potential to affect the lithospheric stress field in Central Europe.
9. The timing of the eruptions close to warming indicates exogenic forcing of endogenic processes. Alternatively, one could also assume that a global period of increased volcanic activity traps geothermal heat under the continental ice sheets and causes their decay.
10. A final potential interpretation could involve the increase/decrease in precipitation and thus the weight of the water in the pore space at the groundwater level or in the maar lake. Maar lakes are known to occur along existing faults, which could be activated by the load of lake level increase of many meters in the case of maar structures without an outlet.

**Supplementary Materials:** The following supporting information can be downloaded at: <https://www.mdpi.com/article/10.3390/quat7020021/s1>, Figure S1: Ulmener Maar Tephra (UMT), 10,650 yr b2k. Photo of UMT in core HM1, sediment petrographic composition and position in the pollen record of HM1; Figure S2: Laacher See Tephra (LST), 13,056 yr b2k; Figure S3: Eltville Tephra (EVT), 24,720 yr b2k; Figure S4: Wartgesberg Tephra (WBT), 28,100 yr b2k; Figure S5: Unknown Tephra 1 (UT1), 30,300 yr b2k; Figure S6: Dreiser-Weiher Tephra (DWT), 40,370 yr b2k; Figure S7: Meerfelder Maar Tephra (MMT), 47,340 yr b2k; Figure S8: Auel Maar Tephra (AUT), 59,130 yr b2k; Figure S9: Schalkenmehrener Maar Tephra (SMT), 72,090 yr b2k; Figure S10: Dehner Maar Tephra (DET), 76,100 yr b2k; Figure S11: Mosenberg Tephra (MOT), 87,590 yr b2k; Figure S12: Chalk Tephra (CHT, former Unknown Tephra 5), 104,050 yr b2k; Figure S13: Dümpelmaar Tephra (DMT), 109,000 yr b2k; Figure S14: Jungferweiher Tephra (JWT), 132,000 yr b2k.

**Author Contributions:** Conceptualization, F.S. (Frank Sirocko); methodology, F.S. (Frank Sirocko), F.K. and M.W.F.; validation, F.K., J.A., S.B., F.S. (Fiona Schenk) and M.W.F.; investigation, F.K., F.S. (Fiona Schenk) and M.W.F.; resources, F.S. (Frank Sirocko); writing—original draft preparation, F.S. (Frank Sirocko); writing—review and editing, F.K., J.A., S.B., F.S. (Fiona Schenk) and M.W.F.; visualization, F.S. (Frank Sirocko), F.K., J.A., S.B. and M.W.F.; supervision, F.S. (Frank Sirocko). All authors have read and agreed to the published version of the manuscript.

**Funding:** This research was funded by the Johannes Gutenberg-University of Mainz.

**Data Availability Statement:** All data will be downloadable at the website ([www.elsa-project.de](http://www.elsa-project.de), accessed on 24 March 2024).

**Acknowledgments:** We are very grateful to the “Stiftung Rheinland-Pfalz für Innovation”, which initiated the first ELSA drilling campaigns. The DEKLIM program of the German Ministry for Education and Research financed many of the ELSA drillings from 2000 to 2005. The “Geocycles” Cluster financed drillings between 2005 and 2012. The final drillings in 2017 took place in cooperation with the Max Planck Institute for Chemistry, headed by Gerald Haug. We thank Petra Sigl for her assistance with the graphical design of the figures. Furthermore, we thank all the reviewers for their valuable comments on the manuscript.

**Conflicts of Interest:** The authors declare no conflicts of interest.

## References

- Büchel, G.; Negendank, J.F.; Wuttke, M.; Viereck-Götte, L. Quartäre und tertiäre Maare der Eifel, Enspel (Westerwald) und Laacher See: Vulkanologie, Sedimentologie und Hydrogeologie. In *Proceedings of the Internationale Maar-Tagung*; Neuffer, F.O., Lutz, H., Eds.; Naturhistorisches Museum Mainz: Mainz, Germany, 2000; pp. 85–112.
- Lorenz, V.; Büchel, G. Zur Vulkanologie der Maare und Schlackenkegel der Westeifel. *Mitt. POLLICHA* **1980**, *68*, 29–100.
- Mertz, H.; Schmincke, H.-U. Mafic potassic lavas of the Quaternary West Eifel volcanic field. *Contrib. Mineral. Petrol.* **1985**, *89*, 330–345. [[CrossRef](#)]
- Meyer, W. *Geologie der Eifel*; Schweizerbart Science Publishers: Stuttgart, Germany, 1998.
- Schmincke, H.-U. The Quaternary Volcanic Fields of the East and West Eifel (Germany); The Quaternary Volcanic Fields of the East and West Eifel (Germany). In *Mantle Plumes: A Multidisciplinary Approach*; Ritter, J.R.R., Christensen, U.R., Eds.; Springer: Berlin/Heidelberg, Germany, 2007; pp. 241–322, ISBN 978-3-540-68046-8.
- Ritter, R.R.; Jordan, M.; Christensen, U.R.; Achauer, U. A mantle plume below the Eifel volcanic fields, Germany. *Earth Planet. Sci. Lett.* **2001**, *186*, 7–14. [[CrossRef](#)]
- Zolitschka, B.; Negendank, J.F.W.; Lottermoser, B.G. Sedimentological proof and dating of the Early Holocene volcanic eruption of Ulmener Maar (Vulkaneifel, Germany). *Geol. Rundsch.* **1995**, *84*, 213–219. [[CrossRef](#)]
- Brauer, A.; Endres, C.; Negendank, J.F.W. Lateglacial calendar year chronology based on annually laminated sediments from Lake Meerfelder Maar, Germany. *Quat. Int.* **1999**, *61*, 17–25. [[CrossRef](#)]
- Sirocko, F.; Seelos, K.; Schaber, K.; Rein, B.; Dreher, F.; Diehl, M.; Lehne, R.; Jäger, K.; Krbetschek, M.; Degering, D. A late Eemian aridity pulse in central Europe during the last glacial inception. *Nature* **2005**, *436*, 833–836. [[CrossRef](#)] [[PubMed](#)]
- Büchel, G. *Vulkanologische Karte West- und Hocheifel*; Johannes Gutenberg University Mainz: Mainz, Germany, 1994.
- Lorenz, V. Formation of phreatomagmatic maar-diatreme volcanoes and its relevance to kimberlite diatremes. *Phys. Chem. Earth* **1975**, *9*, 17–27. [[CrossRef](#)]
- Schmincke, H.U. Phreatomagmatische Phasen in Vulkanen der Osteifel. *Geol. Jahrb.* **1977**, *39*, 3–45.
- Mertz, D.F.; Löhnertz, W.; Nomade, S.; Pereira, A.; Prelević, D.; Renne, P.R. Temporal–spatial evolution of low-SiO<sub>2</sub> volcanism in the Pleistocene West Eifel volcanic field (West Germany) and relationship to upwelling asthenosphere. *J. Geodyn.* **2015**, *88*, 59–79. [[CrossRef](#)]

14. Schnepf, E.; Hradetzky, H. Combined paleointensity and  $^{40}\text{Ar}/^{39}\text{Ar}$  age spectrum data from volcanic rocks of the West Eifel field (Germany): Evidence for an early Brunhes geomagnetic excursion. *J. Geophys. Res. Solid Earth* **1994**, *99*, 9061–9076. [[CrossRef](#)]
15. Schnepf, E. Geomagnetic paleointensities derived from volcanic rocks of the Quaternary East Eifel volcanic field, Germany. *Phys. Earth Planet. Inter.* **1996**, *94*, 23–41. [[CrossRef](#)]
16. van den Bogaard, P.  $^{40}\text{Ar}/^{39}\text{Ar}$  ages of sanidine phenocrysts from Laacher See Tephra (12,900 yr BP): Chronostratigraphic and petrological significance. *Earth Planet. Sci. Lett.* **1995**, *133*, 163–174. [[CrossRef](#)]
17. van den Bogaard, P.; Hall, C.M.; Schmincke, H.-U.; York, D. Precise single-grain  $^{40}\text{Ar}/^{39}\text{Ar}$  dating of a cold to warm climate transition in Central Europe. *Nature* **1989**, *342*, 523–525. [[CrossRef](#)]
18. van den Bogaard, P.; Schmincke, H.U. Die Entwicklungsgeschichte des Mittelrheinraumes und die Eruptionsgeschichte des Osteifel-Vulkanfeldes; Die Entwicklungsgeschichte des Mittelrheinraumes und die Eruptionsgeschichte des Osteifel-Vulkanfeldes. In *Rheingeschichte zwischen Mosel und Maas*; Schirmer, W., Ed.; Deutsche Quartärvereinigung: Hannover, Germany, 1990; Volume 1, pp. 166–190.
19. Lippolt, H.J.; Fuhrmann, U.; Hradetzky, H.  $^{40}\text{Ar}/^{39}\text{Ar}$  age determinations on sanidines of the Eifel volcanic field (Federal Republic of Germany): Constraints on age and duration of a Middle Pleistocene cold period. *Chem. Geol. Isot. Geosci. Sect.* **1986**, *59*, 187–204. [[CrossRef](#)]
20. Sirocko, F.; Dietrich, S.; Veres, D.; Grootes, P.M.; Schaber-Mohr, K.; Seelos, K.; Nadeau, M.-J.; Kromer, B.; Rothacker, L.; Roehner, M.; et al. Multi-proxy dating of Holocene maar lakes and Pleistocene dry maar sediments in the Eifel, Germany. *Quat. Sci. Rev.* **2013**, *62*, 56–76. [[CrossRef](#)]
21. Degering, D.; Krbetschek, M.R. Dating of interglacial sediments by luminescence methods; Dating of interglacial sediments by luminescence methods. In *Developments in Quaternary Sciences*; Elsevier: Amsterdam, The Netherlands, 2007; Volume 7, pp. 157–171, ISBN 978-0-444-52955-8.
22. Britzius, S.; Dreher, F.; Maisel, P.; Sirocko, F. Vegetation Patterns during the Last 132,000 Years: A Synthesis from Twelve Eifel Maar Sediment Cores (Germany): The ELSA-23-Pollen-Stack. *Quaternary* **2024**, *7*, 8. [[CrossRef](#)]
23. Förster, M.W.; Sirocko, F. The ELSA tephra stack: Volcanic activity in the Eifel during the last 500,000 years. *Glob. Planet. Chang.* **2016**, *142*, 100–107. [[CrossRef](#)]
24. Förster, M.W.; Zemlitskaya, A.; Otter, L.M.; Buhre, S.; Sirocko, F. Late Pleistocene Eifel eruptions: Insights from clinopyroxene and glass geochemistry of tephra layers from Eifel Laminated Sediment Archive sediment cores. *J. Quat. Sci.* **2020**, *35*, 186–198. [[CrossRef](#)]
25. Rasmussen, S.O.; Bigler, M.; Blockley, S.P.; Blunier, T.; Buchardt, S.L.; Clausen, H.B.; Cvijanovic, I.; Dahl-Jensen, D.; Johnsen, S.J.; Fischer, H.; et al. A stratigraphic framework for abrupt climatic changes during the Last Glacial period based on three synchronized Greenland ice-core records: Refining and extending the INTIMATE event stratigraphy. *Quat. Sci. Rev.* **2014**, *106*, 14–28. [[CrossRef](#)]
26. Riechelmann, D.F.C.; Albert, J.; Britzius, S.; Krebsbach, F.; Scholz, D.; Schenk, F.; Jochum, K.P.; Sirocko, F. Bioproductivity and vegetation changes documented in Eifel maar lake sediments (western Germany) compared with speleothem growth indicating three warm phases during the last glacial cycle. *Quat. Int.* **2023**, *673*, 1–17. [[CrossRef](#)]
27. Sirocko, F.; Martínez-García, A.; Mudelsee, M.; Albert, J.; Britzius, S.; Christl, M.; Diehl, D.; Diensberg, B.; Friedrich, R.; Fuhrmann, F.; et al. Muted multidecadal climate variability in central Europe during cold stadial periods. *Nat. Geosci.* **2021**, *14*, 651–658. [[CrossRef](#)]
28. Berger, A.; Loutre, M.F. Insolation values for the climate of the last 10 million years. *Quat. Sci. Rev.* **1991**, *10*, 297–317. [[CrossRef](#)]
29. Bereiter, B.; Lüthi, D.; Siegrist, M.; Schüpbach, S.; Stocker, T.F.; Fischer, H. Mode change of millennial  $\text{CO}_2$  variability during the last glacial cycle associated with a bipolar marine carbon seesaw. *Proc. Natl. Acad. Sci. USA* **2012**, *109*, 9755–9760. [[CrossRef](#)] [[PubMed](#)]
30. Korte, M.; Brown, M.C.; Panovska, S.; Wardinski, I. Robust Characteristics of the Laschamp and Mono Lake Geomagnetic Excursions: Results From Global Field Models. *Front. Earth Sci.* **2019**, *7*, 86. [[CrossRef](#)]
31. Muscheler, R.; Beer, J.; Kubik, P.W.; Synal, H.-A. Geomagnetic field intensity during the last 60,000 years based on  $^{10}\text{Be}$  and  $^{36}\text{Cl}$  from the Summit ice cores and  $^{14}\text{C}$ . *Quat. Sci. Rev.* **2005**, *24*, 1849–1860. [[CrossRef](#)]
32. Jouzel, J.; Masson-Delmotte, V.; Cattani, O.; Dreyfus, G.; Falourd, S.; Hoffmann, G.; Minster, B.; Nouet, J.; Barnola, J.M.; Chappellaz, J.; et al. Orbital and Millennial Antarctic Climate Variability over the Past 800,000 Years. *Science* **2007**, *317*, 793–796. [[CrossRef](#)] [[PubMed](#)]
33. Martrat, B.; Grimalt, J.O.; Shackleton, N.J.; de Abreu, L.; Hutterli, M.A.; Stocker, T.F. Four Climate Cycles of Recurring Deep and Surface Water Destabilizations on the Iberian Margin. *Science* **2007**, *317*, 502–507. [[CrossRef](#)]
34. Lisiecki, L.E.; Raymo, M.E. A Pliocene-Pleistocene stack of 57 globally distributed benthic  $\delta^{18}\text{O}$  records. *Paleoceanography* **2005**, *20*, 2004PA001071. [[CrossRef](#)]
35. Grant, K.M.; Rohling, E.J.; Ramsey, C.B.; Cheng, H.; Edwards, R.L.; Florindo, F.; Heslop, D.; Marra, F.; Roberts, A.P.; Tamisiea, M.E.; et al. Sea-level variability over five glacial cycles. *Nat. Commun.* **2014**, *5*, 5076. [[CrossRef](#)]
36. Siddall, M.; Rohling, E.J.; Almogi-Labin, A.; Hemleben, C.; Meischner, D.; Schmelzer, I.; Smeed, D.A. Sea level fluctuations during the last glacial cycle. *Nature* **2003**, *423*, 853–858. [[CrossRef](#)]
37. Lambeck, K.; Purcell, A. *Glacial Rebound and Crustal Stress in Finland*; Posiva: Eurajoki, Finland, 2003; ISBN 951-652-124-X.

38. Wu, P.; Johnston, P.; Lambeck, K. Postglacial rebound and fault instability in Fennoscandia. *Geophys. J. Int.* **1999**, *139*, 657–670. [[CrossRef](#)]
39. Wang, C.-Y.; Manga, M. Earthquakes Influenced by Water; Earthquakes Influenced by Water. In *Water and Earthquakes*; Wang, C.-Y., Manga, M., Eds.; Lecture Notes in Earth System Sciences; Springer: Cham, Switzerland, 2021; pp. 61–82, ISBN 978-3-030-64308-9.
40. Carlson, G.; Shirzaei, M.; Werth, S.; Zhai, G.; Ojha, C. Seasonal and Long-Term Groundwater Unloading in the Central Valley Modifies Crustal Stress. *J. Geophys. Res. Solid Earth* **2020**, *125*, e2019JB018490. [[CrossRef](#)]
41. Rasmussen, S.O.; Andersen, K.K.; Svensson, A.M.; Steffensen, J.P.; Vinther, B.M.; Clausen, H.B.; Siggaard-Andersen, M.-L.; Johnsen, S.J.; Larsen, L.B.; Dahl-Jensen, D.; et al. A new Greenland ice core chronology for the last glacial termination. *J. Geophys. Res.* **2006**, *111*, 1–16. [[CrossRef](#)]
42. Reinig, F.; Wacker, L.; Jöris, O.; Oppenheimer, C.; Guidobaldi, G.; Nievergelt, D.; Adolphi, F.; Cherubini, P.; Engels, S.; Esper, J.; et al. Precise date for the Laacher See eruption synchronizes the Younger Dryas. *Nature* **2021**, *595*, 66–69. [[CrossRef](#)] [[PubMed](#)]
43. Schmidt, C.; Schaarschmidt, M.; Kolb, T.; Büchel, G.; Richter, D.; Zöller, L. Luminescence dating of Late Pleistocene eruptions in the Eifel Volcanic Field, Germany. *J. Quat. Sci.* **2017**, *32*, 628–638. [[CrossRef](#)]
44. Schaber, K.; Sirocko, F. Lithologie und Stratigraphie der spätpleistozänen Trockenmaare der Eifel. *Mainz. Geowiss. Mitteilungen* **2005**, *33*, 295–340.
45. Büchel, G. Maars of the Westeifel, Germany; Maars of the Westeifel, Germany. In *Paleolimnology of European Maar Lakes*; Negendank, J.F.W., Zolitschka, B., Eds.; Lecture Notes in Earth Sciences; Springer: Berlin/Heidelberg, Germany, 1993; Volume 49, pp. 1–13, ISBN 978-3-540-56570-3.
46. van den Bogaard, P.; Schmincke, H.-U. The eruptive center of the late quaternary Laacher see tephra. *Geol. Rundsch.* **1984**, *73*, 933–980. [[CrossRef](#)]
47. Jouannic, G.; Walter-Simonnet, A.V.; Bossuet, G.; Simonnet, J.P.; Jacotot, A. Evidence of tephra reworking in loess based on 2D magnetic susceptibility mapping: A case study from Rocourt, Belgium. *Quat. Int.* **2016**, *394*, 123–132. [[CrossRef](#)]
48. Zens, J.; Zeeden, C.; Römer, W.; Fuchs, M.; Klasen, N.; Lehmkuhl, F. The Eltville Tephra (Western Europe) age revised: Integrating stratigraphic and dating information from different Last Glacial loess localities. *Palaeogeogr. Palaeoclimatol. Palaeoecol.* **2017**, *466*, 240–251. [[CrossRef](#)]
49. Eichhorn, L.; Pirrung, M.; Zolitschka, B.; Büchel, G. Pleniglacial sedimentation process reconstruction on laminated lacustrine sediments from lava-dammed Paleolake Alf, West Eifel Volcanic Field (Germany). *Quat. Sci. Rev.* **2017**, *172*, 83–95. [[CrossRef](#)]
50. Schenk, F.; Hambach, U.; Britzius, S.; Veres, D.; Sirocko, F. A Cryptotephra Layer in Sediments of an Infilled Maar Lake from the Eifel (Germany): First Evidence of Campanian Ignimbrite Ash Airfall in Central Europe. *Quaternary* **2024**, *7*, 17. [[CrossRef](#)]
51. Zöller, L.; Blanchard, H. The partial heat—Longest plateau technique: Testing TL dating of Middle and Upper Quaternary volcanic eruptions in the Eifel Area, Germany. *EG Quat. Sci. J.* **2009**, *58*, 86–106. [[CrossRef](#)]

**Disclaimer/Publisher’s Note:** The statements, opinions and data contained in all publications are solely those of the individual author(s) and contributor(s) and not of MDPI and/or the editor(s). MDPI and/or the editor(s) disclaim responsibility for any injury to people or property resulting from any ideas, methods, instructions or products referred to in the content.